Genomic investigation of the strawberry pathogen *Phytophthora fragariae* indicates pathogenicity is associated with transcriptional variation in three key races

Thomas M. Adams[1,2]¤, Andrew D. Armitage[1], Maria K. Sobczyk[1]†, Helen J. Bates[1], Javier F. Tabima[3], Brent A. Kronmiller[4], Brett M. Tyler[3,4], Niklaus J. Grünwald[5], Jim M. Dunwell[2], Charlotte F. Nellist[1]* and Richard J. Harrison[1,6]

[1]Department of Genetics, Genomics and Breeding, NIAB EMR, New Road, East Malling, Kent, ME19 6BJ, UK.

[2]School of Agriculture, Policy and Development, University of Reading, Reading, Berkshire, RG6 6AH, UK.

[3]Department of Botany and Plant Pathology, Center for Genome Biology and Biocomputing, Oregon State University, Corvallis, OR, USA.

[4]Center for Genome Biology and Biocomputing, Oregon State University, Corvallis, OR, 97331, USA.

[5]Horticultural Crops Research Unit, Agricultural Research Service, United States Department of Agriculture, Corvallis, OR, USA.

[6] NIAB Cambridge Crop Research, NIAB, Huntingdon Road, Cambridge, CB3 0LE, UK.

¤ Current address: Department of Crop Genetics, John Innes Centre, Norwich Research Park, Norwich, NR4 7UH, UK.

† Current address: University of Bristol, Oakfield House, Oakfield Grove, Clifton, BS8 2BN, UK.

*Correspondence:

Charlotte F. Nellist

charlotte.nellist@emr.ac.uk

ABSTRACT

The oomycete *Phytophthora fragariae* is a highly destructive pathogen of cultivated strawberry (*Fragaria × ananassa*), causing the root rotting disease, 'red core'. The host-pathogen interaction has a well described gene-for-gene resistance relationship, but to date neither candidate avirulence nor resistance genes have been identified. We sequenced a set of American, Canadian and UK isolates of known race type, along with three representatives of the closely related pathogen of the raspberry (*Rubus idaeus*), *Phytophthora rubi*, and found a clear population structure, with a high degree of nucleotide divergence seen between some race types and abundant private variation associated with race types 4 and 5. In contrast, between isolates defined as UK races 1, 2 & 3 (UK1-2-3) there was no evidence of gene loss or gain; or the presence of insertions/deletions (INDELs) or Single Nucleotide Polymorphisms (SNPs) within or in proximity to putative pathogenicity genes could be found associated with race variation. Transcriptomic analysis of representative UK1-2-3 isolates revealed abundant expression variation in key effector family genes associated with pathogen race; however, further long read sequencing did not reveal any long range polymorphisms to be associated with avirulence to race UK2 or UK3 resistance, suggesting either control in *trans* or other stable forms of epigenetic modification modulating gene expression. This work reveals the combined power of population resequencing to uncover race structure in pathosystems and *in planta* transcriptomic analysis to identify candidate avirulence genes. This work has implications for the identification of putative avirulence genes in the absence of associated expression data and points towards the need for detailed molecular characterisation of mechanisms of effector regulation and silencing in oomycete plant pathogens.

INTRODUCTION

Phytophthora fragariae, the causal agent of red core or red stele root rot, is a highly destructive pathogen of cultivated strawberry (*Fragaria × ananassa*), resulting in whole plant collapse. The majority of commercial strawberries grown in the UK are grown on table tops using soilless substrate, under polytunnels or in glasshouses (Robinson Boyer et al., 2016). *Phytophthora* spp. are a particular problem in these systems due to the ease of spread through the irrigation system via the motile zoospores. Since the first report in Scotland in 1920, this disease has spread to the majority of strawberry growing regions, except China and the Southern Mediterranean regions of Europe (van de Weg, 1997b; EFSA Panel on Plant Health (PLH), 2014). Currently, it is treated as a quarantine pest by the European and Mediterranean Plant Protection Organization (EPPO), where it is listed as an A2

2

60   pest (van de Weg, 1997b; EPPO, 2018). The classification of this pathogen has proven controversial,

61   as initially the organism was identified as a single species (Hickman, 1941), but when a *Phytophthora*

62   disease of raspberry (*Rubus idaeus*) was discovered, it was reclassified as *P. fragariae* var. *fragariae*

63   (Wilcox et al., 1993). More recently, the pathogens have been separated into distinct species, *P.*

64   *fragariae* and *Phytophthora rubi*, affecting strawberry and raspberry respectively. This was supported

65   by sequence analysis of key loci (Man in 't Veld, 2007), as well as whole genome analyses (Tabima

66   et al., 2018).

67   It has previously been proposed that the ability of different isolates of *P. fragariae* to cause

68   disease on a variety of *F. × ananassa* cultivars can be explained by a gene-for-gene model (van de

69   Weg, 1997a). The model is currently thought to consist of at least eleven resistance genes in *F. ×*

70   *ananassa* with eleven corresponding avirulence factors in *P. fragariae* (W. E. van de Weg,

71   Wageningen University and Research, The Netherlands, personal communication). The development

72   of race schemes is country dependent and ones exist for the UK, USA and Canada.

73   All publicly available genome assemblies of *P. fragariae* have to date solely utilised Illumina

74   short read sequencing technologies, resulting in assemblies of 73.68 Mb and 76 Mb, in 1,616 and

75   8,511 scaffolds respectively (Gao et al., 2015; Tabima et al., 2017). Recently, long read sequencing

76   technology has been shown to provide assemblies of improved contiguity for *Phytophthora*

77   pathogens, specifically the generation of the haplotype-phased assembly of *Phytophthora ramorum*

78   (60.5 Mb in 302 primary contigs) using PacBio sequencing (Malar et al., 2019) and the assembly of

79   *Phytophthora capsici* (95.2 Mb in 424 scaffolds) using Oxford Nanopore Technology (Cui et al.,

80   2019).

81   Pathogenomic investigations in *Phytophthora* species of pathosystems with similar gene-for-

82   gene models of resistance have shown a variety of mechanisms through which variation in virulence

83   can be controlled. For instance, in *Phytophthora sojae*, the *Avr1d* gene was identified as an RxLR

84   effector recognised by the *Rps1d* resistance gene in soybean (Yin et al., 2013). Studies of the RxLR

85   effector *PiAvr4* from *Phytophthora infestans* showed that it was always present in isolates avirulent

86   on potato plants containing the resistance gene *R4*, whereas virulent isolates possessed a frameshift

87   mutation producing a truncated protein (van Poppel et al., 2008). In comparison, *Avr3c* in *P. sojae*

88   was identified in both virulent and avirulent isolates on soybean plants containing *Rps3c*, but in

89   virulent isolates the gene displayed several polymorphisms resulting in a change to the amino acid

90   sequence leading to a failure of recognition by the plant (Dong et al., 2009). Recently, investigations

91   of the EC-1 clonal lineage of *P. infestans* revealed a variation of the ability of isolates to cause disease

92   on potato plants possessing the *Rpi-vnt1.1* gene. It was shown, in the absence of genetic mutations,

93   that differences in the expression level of *Avrvnt1* were detected and these correlated with virulence

94   (Pais et al., 2018).

95   In this study, we assembled and annotated a population of isolates of *P. fragariae* and the

96   related pathogen of raspberry, *P. rubi*. We identified a subpopulation of *P. fragariae* isolates

97   representing three distinct pathogenicity races (UK1-2-3). This subpopulation was found to be

98   remarkably similar in gene complement, as well as showing little divergence at the nucleotide

99   sequence level. To further investigate the cause of the observed variation in pathogenicity phenotypes,

100   transcriptomic datasets were generated for representative isolates of each pathogenicity race in this

101   subpopulation. This revealed expression level polymorphisms between the isolates, allowing for the

102   generation of candidate lists for *PfAvr1*, *PfAvr2* and *PfAvr3*. A strong candidate for *PfAvr2*,

103   PF003_g27513 was identified as expressed in the BC-16 and A4 (UK2) isolates, yet not expressed in

104   the BC-1 (UK1) and NOV-9 (UK3) isolates. A candidate for *PfAvr3* was also identified,

105   PF009_g26276; it is expressed in NOV-9 (UK3), yet not expressed in BC-1 (UK1), A4 (UK2) and

106   BC-16 (UK2) isolates. Additional sequencing did not reveal long-range polymorphisms influencing

107   the expression of these candidate genes; we therefore suggest control may be in *trans* or due to

108   epigenetic factors.

109

110   **MATERIALS AND METHODS**

111   **Isolate selection and sources**

112   A selection of ten isolates of *P. fragariae* were sourced from the Atlantic Food and Horticulture

113   Research Centre (AFHRC), Nova Scotia, Canada. An additional isolate of *P. fragariae*, SCRP245,

114   alongside three *P. rubi* isolates, were sourced from the James Hutton Institute (JHI), Dundee, Scotland

115   (detailed in **Table 1**).

116   **Culturing of isolates**

117   All work with *P. fragariae* and *P. rubi* was conducted in a Tri-MAT Class-II microbiological safety

118   cabinet. Isolates were routinely subcultured on kidney bean agar (KBA) produced as previously

119   described (Maas, 1972). Isolates were grown by transferring two pieces of between 1 and 4 mm^2 onto

120   fresh KBA plates, subsequently sealed with Parafilm®. Plates were then grown at 20°C in the dark in

121   a Panasonic MIR-254 cooled incubator for between seven and fourteen days.

122   Mycelia were also grown in liquid pea broth, produced as previously described (Campbell et
123   al., 1989) with the addition of 10 g/L sucrose. These plates were inoculated with five pieces (1 - 4
124   mm^2) of mycelium and media, subsequently sealed with Parafilm®. These were grown at 20 °C for
125   four to five days in constant darkness.

Pathogenicity testing of isolates

127   Mother stock plants of *F. × ananassa* were maintained in 1 L pots in polytunnels. Runner plants were
128   pinned down into 9 cm diameter pots filled with autoclaved 1:1 peat-based compost:sand. The clones
129   were grown on for three weeks to establish their own root system and then were cut from the mother
130   plant. Inoculations were performed as described previously (van de Weg et al., 1996). Plants were
131   placed in a growth chamber with 16/8 hour light/dark cycle at a constant 15 °C. Inoculated plants
132   stood in a shallow layer of tap water (2 - 7 mm) for the entire experiment and were watered from
133   above twice a week. After six weeks, plants were dug up and the roots were rinsed to remove the
134   soil/sand mix. Roots were then assessed for distinctive disease symptoms of 'rat's tails', which is the
135   dieback from the root tip and 'red core', which is the red discolouration of the internal root visible
136   when longitudinally sliced open. Samples for which infection was unclear were visualised under a
137   light microscope for the presence of oospores. This was performed through squash-mounting of the
138   root tissue, where a sample of root was excised and pressed between a microscope slide and cover
139   slip. This sample was then examined at 40x magnification under high light intensity with a Leitz
140   Dialux 20 light microscope.

Sequencing of DNA

142   For Illumina sequencing, gDNA was extracted from 300 mg of freeze-dried mycelium using the
143   Macherey-Nagel NucleoSpin® Plant II Kit. The manufacturer's protocol was modified by doubling
144   the amount of lysis buffer PL1 used, increasing the incubation following RNase A addition by five
145   minutes, doubling the volume of buffer PC and eluting in two steps with 35 μL of buffer PE warmed
146   to 70 °C. For PacBio and Oxford Nanopore Technologies (ONT) sequencing, gDNA was extracted
147   using the Genomic-Tip DNA 100/G extraction kit, following the Tissue Sample method.
148   To create Illumina PCR-free libraries, DNA was sonicated using a Covaris M220 and size-
149   selected using a BluePippin BDF1510 1.5% gel selecting for 550 bp. Libraries were constructed using
150   the NEBNext enzymes: End repair module (E6050), A-TAiling module (E6053), Blunt T/A ligase
151   (M0367) and Illumina single-indexed adapters. Sequencing was performed to generate 2 x 300 bp

152 reads on a MiSeq^{TM} system using MiSeq Reagent Kit V3 600 cycle (MS-102-3003). PacBio library

153 preparation and sequencing was performed by the Earlham Institute, UK on a PacBio RS II machine.

154 ONT sequencing libraries were created using the SQK-LSK108 kit following the manufacturer's

155 protocol and sequenced using the FAH69834 FLO-MIN106 flow cell on a GridION for approximately

156 28 hours.

Inoculation time course experiment

158 Growth of isolates for inoculations were performed on fresh KBA plates for approximately 14 days

159 as described above, before the mycelium had reached the plate edge. Plugs of mycelium growing on

160 agar were taken using a flame sterilised 10 mm diameter cork borer and plugs were submerged in

161 chilled stream water. Plates were incubated in constant light for three days at 13 °C, with the water

162 changed every 24 hours. For the final 24 hours, chilled Petri's solution (Judelson et al., 1993) was

163 used. Roots of micropropagated *F. × ananassa* 'Hapil' plants (GenTech, Dundee, UK), maintained

164 on *Arabidopsis thaliana* salts (ATS) media (Taylor et al., 2016), were submerged for one hour before

165 transfering back to ATS plates. These plates were kept at 15 °C, with 16/8 hour light/dark cycle, with

166 a photosynthetic photon flux (PPF) of 150 μmol m^{-2} s^{-1} provided by fluorescent lamps

167 (FL40SSENW37), in a Panasonic MLR-325H controlled environment chamber. Root tissue was

168 harvested at a selection of time points post inoculation by rinsing root tissue successively in three

169 beakers of sterile dH$_2$O to remove all media. Roots were separated below the crown tissue, flash frozen

170 in liquid nitrogen and stored at -80 °C.

171 Extraction of total RNA from inoculated root tissue was performed similarly to the previously

172 described 3% CTAB$_3$ method (Yu et al., 2012). Briefly, plant material was disrupted under liquid

173 nitrogen in a mortar and pestle, previously decontaminated through cleaning with RNaseZap^{TM}

174 solution and baking for 2 hours at 230 °C to deactivate RNAse enzymes. This material was transferred

175 to a warmed extraction buffer (Yu et al., 2012) containing β-mercaptoethanol with 0.01 g of PVPP

176 added per 0.1 g of frozen tissue. The remaining steps were performed as previously described (Yu et

177 al., 2012), except that 60 μL DEPC-treated H$_2$O was used to elute RNA.

178 Mycelium was grown in liquid pea both and dried on a Q100 90 mm filter paper (Fisher

179 Scientific) using a Büchner funnel and a Büchner flask attached to a vacuum pump. Total RNA was

180 then extracted using the QIAGEN RNEasy Plant Mini kit with the RLC buffer. Extraction was carried

181 out following the manufacturer's instructions with an additional spin to remove residual ethanol.

6

182   RNA was checked for quality using a NanoDrop 1000 spectrophotometer, quantity with a

183   Qubit 2.0 Fluorometer and integrity with a TapeStation 4200 before being prepared for sequencing

184   via Reverse Transcription-Polymerase Chain Reaction (RT-PCR) and sequencing on an Illumina

185   HiSeq^{TM} 4000 by Novogene, Hong Kong, Special Administrative Region, China. Timepoints for

186   sequencing were selected through the detection of β-tubulin transcripts by RT-PCR. Reverse

187   transcription was performed with the SuperScript^{TM} III Reverse Transcriptase kit with an equal

188   amount of RNA used for each sample. The complementary DNA (cDNA) was then analysed by PCR

189   with 200 μM dNTPs, 0.2 μM of each primer (detailed in **Supplementary Table S1**), 2 μL of cDNA

190   template and 2.5 units of Taq DNA polymerase and the buffer supplied in a 20 μL reaction. Reactions

191   were conducted in a Veriti 96-well thermocycler with an initial denaturation step at 95 °C for 30

192   seconds, followed by 35 cycles of a denaturation step at 95 °C for 30 seconds, an annealing

193   temperature of 60 °C for 30 seconds and an extension step of 72 °C for 30 seconds. This was followed

194   by a final extension step of 72 °C for 5 minutes and held at 10 °C. Products were visualised by gel

195   electrophoresis on a 1% w/v agarose gel at 80 V for 90 minutes, stained with GelRed. Following this,

196   three biological replicates of samples taken at: 24 hpi, 48 hpi and 96 hpi for BC-16, 48 hpi for BC-1

197   and 72 hpi for NOV-9 were sequenced (**Supplementary Figure S1**). Additionally, *in vitro* mycelial

198   RNA was sequenced.

199   *P. rubi* RNA-Seq reads were sequenced on a HiSeq^{TM} 2000 system.

Genome assembly

201   Prior to assembly, Illumina reads were cleaned and sequencing adaptors were removed with fastq-mcf

202   (Aronesty, 2013). Quality control of PacBio data was performed by the Earlham Institute, Norwich,

203   UK. ONT reads were basecalled with Albacore version 2.2.7 and adaptors were removed with

204   Porechop version 0.2.0 (Wick, 2018) and the trimmed reads were corrected with Canu version 1.4

205   (Koren et al., 2017).

206   Assemblies of isolates sequenced solely with Illumina data were generated with SPAdes

207   version 3.11.0 (Bankevich et al., 2012) with Kmer sizes of 21, 33, 55, 77, 99 and 127. PacBio reads

208   were assembled using FALCON-Unzip (Chin et al., 2016). FALCON version

209   0.7+git.7a6ac0d8e8492c64733a997d72a9359e1275bb57 was used, followed by FALCON-Unzip

210   version 0.4.0 and Quiver (Chin et al., 2013). Error corrected ONT reads were assembled using

211   SMARTdenovo version 1.0.0 (Ruan, 2018).

212   Following assembly, error correction was performed on ONT assemblies by aligning the reads

213   to the assembly with Minimap2 version 2.8r711-dirty (Li, 2018) to inform ten iterations of Racon

214   version 1.3.1 (Vaser et al., 2017). Following this, reads were again mapped to the assembly and errors

215   were corrected with Nanopolish version 0.9.0 (Simpson, 2018). PacBio and ONT assemblies had

216   Illumina reads mapped with Bowtie 2 version 2.2.6 (Langmead and Salzberg, 2012) and SAMtools

217   version 1.5 (Li et al., 2009) to allow for error correction with ten iterations of Pilon version 1.17

218   (Walker et al., 2014).

219   Following assembly, all contigs smaller than 500 bp were discarded and assembly statistics

220   were collected using Quast version 3.0 (Gurevich et al., 2013). BUSCO statistics were collected with

221   BUSCO version 3.0.1 (Simão et al., 2015) using the eukaryota_odb9 database on the assemblies, as

222   the stramenopile database was not available at the time of the analysis. Identification of repetitive

223   sequences was performed with Repeatmasker version open-4.0.5 (Smit et al., 2015) and

224   RepeatModeler version 1.73 (Smit and Hubley, 2015). Transposon related sequences were identified

225   with TransposonPSI release 22nd August 2010 (Haas, 2010).

Prediction of gene models and effectors

227   Gene and effector prediction was performed similarly to a previously described method (Armitage et

228   al., 2018). Firstly, raw RNA-Seq reads of BC-16 from both mycelial samples and the inoculation time

229   course were cleaned with fastq-mcf (Aronesty, 2013). Reads from the inoculation time course were

230   first aligned to the *Fragaria vesca* version 1.1 genome (Shulaev et al., 2011) with STAR version

231   2.5.3a (Dobin et al., 2013) and unmapped reads were kept. These unmapped reads and those from *in*

232   *vitro* mycelium were mapped to the assembled *P. fragariae* genomes with STAR (Dobin et al., 2013).

233   RNA-Seq data from *P. rubi* were aligned to *P. rubi* assemblies with the same method. Further steps

234   were performed as previously described (Armitage et al., 2018). Additionally, putative apoplastic

235   effectors were identified through the use of ApoplastP (Sperschneider et al., 2018). Statistical

236   significance of the differences between predicted numbers of effector genes was assessed with a

237   Welch two sample t-test in R version 3.4.3 (R core team, 2017).

Gene orthology analysis

239   Orthologue identification was performed using OrthoFinder version 1.1.10 (Emms and Kelly, 2015)

240   on predicted proteins from all sequenced *P. fragariae* and *P. rubi* isolates. Orthogroups were

241   investigated for expanded and unique groups for races UK1, UK2 and UK3. Unique orthogroups were

242 those containing proteins from only one race and expanded orthogroups were those containing more
243 proteins from a specific race than other races. Venn diagrams were created with the VennDiagram R
244 package version 1.6.20 (Chen and Boutros, 2011) in R version 3.2.5 (R Core Team, 2016).

Identification and analysis of variant sites and population structure

246 Variant sites were identified through the use of the GATK version 3.6 HaplotypeCaller in diploid
247 mode (McKenna et al., 2010) following alignment of Illumina reads for all sequenced isolates to the
248 FALCON-Unzip assembled genome with Bowtie 2 version 2.2.6 (Langmead and Salzberg, 2012) and
249 filtered with vcflib (Garrison, 2012) and VCFTools (Danecek et al., 2011). Additionally, structural
250 variants were identified with SvABA (Wala et al., 2018) following the alignment of Illumina reads
251 from all sequenced isolates to the FALCON-Unzip assembled genome with BWA-mem version 0.7.15
252 (Li, 2013). Population structure was assessed with fastSTRUCTURE (Raj et al., 2014) following
253 conversion of the input file with Plink version 1.90 beta (Purcell et al., 2007). Finally, a custom Python
254 script was used to identify variant sites private to races UK1, UK2 or UK3 (see Availability of
255 Computer Code below).

Assessment of gene expression levels and the identification of candidate avirulence genes

258 RNA-Seq reads of BC-1, BC-16 and NOV-9 were aligned to the assembled genomes of BC-1, BC-16
259 and NOV-9 as described above. Expression levels and differentially expressed genes were identified
260 with featureCounts version 1.5.2 (Liao et al., 2014) and the DESeq2 version 1.10.1 R package (Love
261 et al., 2014). Multiple test correction was performed as part of the analysis within the DESeq2
262 package.

263   Candidate avirulence genes were identified through the analysis of uniquely expressed genes
264 and uniquely differentially expressed genes for each of the three isolates. Uniquely expressed genes
265 were those with a Fragments Per Kilobase of transcript per Million mapped reads (FPKM) value
266 greater than or equal to 5 in any time point from the inoculation time course experiment for a single
267 isolate. Uniquely differentially expressed genes were those with a minimum LFC of 3 and a *p*-value
268 threshold of 0.05. Genes were compared between isolates through the use of orthology group
269 assignments described above and scored on a one to six scale, with five and six deemed high
270 confidence and one and two deemed as low confidence.

271   To identify homologous genes in other *Phytophthora* spp., candidate RxLRs were processed

272 by SignalP-5.0 (Armenteros et al., 2019) to identify the cleavage site. The signal peptide sequence

273 was removed before being submitted for a tblastn (Altschul et al., 1997) search on GenBank;

274 interesting top hits are reported.

275   The expression levels of a strong candidate *PfAvr2* gene, PF003_g27513 and a candidate

276 *PfAvr3* gene, PF009_g26276, were assessed via RT-qPCR. RNA-Seq results for reference genes

277 identified previously in *Phytophthora parasitica* (Yan and Liou, 2006) were examined for stability of

278 expression levels, resulting in the selection of β-tubulin (PF003_g4288) and WS41 (PF003_g28439)

279 as reference genes. Primers were designed using the modified Primer3 version 2.3.7 implemented in

280 Geneious R10 (Untergasser et al., 2012). Reverse transcription was performed on three biological

281 replicates of each sequenced timepoint, alongside: 24 hpi, 72 hpi and 96 hpi for BC-1 and 24 hpi, 48

282 hpi and 96 hpi for NOV-9 with the QuantiTect Reverse Transcription Kit. Quantitative PCR (qPCR)

283 was then performed in a CFX96^{TM} Real-Time PCR detection system in 10 μL reactions of: 5 μL of

284 2x qPCRBIO SyGreen Mix Lo-Rox, 2 μL of a 1:3 dilution of the cDNA sample in dH$_2$O and 0.4 μL

285 of each 10 μM primer and 2.2 μL dH$_2$O. The reaction was run with the following conditions: 95 °C

286 for 3 minutes, 39 cycles of 95 °C for 10 seconds, 62 °C for 10 seconds and 72 °C for 30 seconds. This

287 was followed by 95 °C for 10 seconds, and a 5 second step ranging from 65 °C to 95 °C by 0.5 °C

288 every cycle. At least two technical replicates for each sample were performed and the melt curve

289 results were analysed to ensure the correct product was detected. Relative gene expression was

290 calculated using the comparative cycle threshold (C_T) method (Livak and Schmittgen, 2001). Where

291 there was a difference of at least 1 C_T value between the minimum and maximum results for technical

292 replicates, further reactions were conducted. Outlier technical replicates were first identified as being

293 outside 1.5 times the interquartile range. Following this, additional outliers were identified using the

294 Grubb's test and excluded from the analysis. Technical replicates were averaged for each biological

295 replicate and expression values were calculated as the mean of the three biological replicates.

296 **Investigation of *cis* and *trans* variations for strong candidate avirulence gene**

297 The regions upstream and downstream of PF003_g27513 and PF009_g26276 in the FALCON-Unzip

298 assembly of BC-16 and the SMARTdenovo assembly of NOV-9 were aligned with MAFFT in

299 Geneious R10 (Katoh et al., 2002; Katoh and Standley, 2013). Variant sites were identified through

300 visual inspection of the alignment alongside visualisation of aligned short reads from BC-16 and

301 NOV-9 to both assemblies with Bowtie 2 version 2.2.6 (Langmead and Salzberg, 2012) in IGV

302 (Thorvaldsdóttir et al., 2013).

303   Transcription factors were identified with a previously described HMM of transcription factors

304 and transcriptional regulators in Stramenopiles (Buitrago-Flórez et al., 2014). These proteins were

305 then analysed through methods described above for gene loss or gain, nearby variant sites and

306 differential expression between isolates.

Availability of computer code

308 All computer code is available at:

309 https://github.com/harrisonlab/phytophthora_fragariae,

310 https://github.com/harrisonlab/phytophthora_rubi   and

311 https://github.com/harrisonlab/popgen/blob/master/snp/vcf_find_difference_pop.py.

312

313 **RESULTS**

314 **Race typing allowed standardisation of US and UK race nomenclature**

315 The *P. fragariae* isolates A4 (race US4), BC-1 (race CA1), BC-16 (race CA3), NOV-5 (race CA1),

316 NOV-9 (race CA2), NOV-27 (race CA2) and NOV-71 (race CA2) (**Table 1**) were phenotyped on a

317 differential series of four *F. × ananassa* cultivars with known resistance. These were: 'Allstar'

318 (containing *Rpf1*, *Rpf2* and *Rpf3*), 'Cambridge Vigour' (containing *Rpf2* and *Rpf3*), 'Hapil'

319 (containing no resistance genes) and 'Redgauntlet' (containing *Rpf2*) (van de Weg et al., 1996; R.

320 Harrison, unpublished). Following assessment of below ground symptoms, it was shown that race

321 CA1 was equivalent to UK1, race CA2 was equivalent to UK3, race CA3 was equivalent to UK2 and

322 race US4 was equivalent to UK2 (**Figure 1; Table 2**).

323 **A highly contiguous genome assembly of BC-16**

324 Long read PacBio sequencing generated a highly contiguous *P. fragariae* isolate BC-16 (UK2)

325 reference genome of 91 Mb in 180 contigs with an N50 value of 923.5 kb (**Table 3**). This was slightly

326 larger than the closely related, well studied species from Clade 7, *P. sojae*, at 83 Mb (**Table 3**; Tyler

327 et al., 2006). The BC-16 assembly contained 266 of 303 eukaryotic Benchmarking Universal Single-

328 Copy Orthologs (BUSCO) genes (**Table 4**), compared to 270 in *P. sojae* (Armitage et al., 2018) and

329 so likely represented a similar completeness of the genome as the *P. sojae* assembly. The *P. fragariae*

11

330   genome was shown to be highly repeat rich, with 38% of the assembly identified as repetitive or low

331   complexity, a larger value than the 29% shown for *P. sojae* (Armitage et al., 2018). A total of 37,049

332   genes encoding 37,346 proteins were predicted in the BC-16 assembly, consistening of 20,222 genes

333   predicted by BRAKER1 (Hoff et al., 2016) and 17,131 additional genes added from CodingQuarry

334   (Testa et al., 2015). From these gene models, 486 putative RxLR effectors, 82 putatitve crinkler

335   effectors (CRNs) and 1,274 putative apoplastic effectors were identified (**Table 5**). Additionally, a

336   total of 4,054 low confidence gene models were added from intergenic ORFs identified as putative

337   effectors. These consisted of 566 putative RxLRs, 5 putative CRNs and 3,483 putatitve apoplastic

338   effectors. This resulted in a combined total of 41,103 genes encoding 41,400 proteins with 1,052

339   putative RxLRs, 85 putative CRNs and 4,757 putative apoplastic effectors (**Table 3** and **Table 5**).

340   **A comparable number of effector genes were identified through resequencing of isolates of**

341   ***Phytophthora fragariae* and *Phytophthora rubi***

342   Ten isolates of *P. fragariae* and three isolates of *P. rubi* were additionally resequenced, *de novo*

343   assembled and annotated (**Table 1** and **Table 4**). These isolates showed similar assembly statistics

344   within and between species; an average of 79 Mb in 12,804 contigs with an N50 of 19.3 kb in *P.*

345   *fragariae*, compared to an average of 78 Mb in 13,882 contigs with an N50 of 16.8 kb in *P. rubi*. All

346   assemblies showed 31% of the assembly was identified as repetitive or low complexity sequences. On

347   average both *P. fragariae* and *P. rubi* showed high levels of completeness, with an average of 274/303

348   BUSCO genes identified as single copies in these assemblies. Interestingly, a total of 17 genes were

349   consistently not identified in Illumina, PacBio and Nanopore assemblies of *P. fragariae* and *P. rubi*

350   isolates, suggesting these genes may be absent from these species and as such may not be considered

351   true eukaryotic BUSCO genes. An average of 67 CRNs were predicted in *P. fragariae* and an average

352   of 118 CRNs in *P. rubi*. A significantly ($p = 0.013$) smaller number of RxLRs were predicted in *P.*

353   *rubi* isolates than *P. fragariae* isolates alongside a significantly ($p = 0.039$) smaller number of

354   apoplastic effectors predicted in *P. rubi* than *P. fragariae* (**Table 5**). However, it is important to note

355   that these effectors were predicted from a subset of secreted proteins, of which there were significantly

356   ($p = 0.030$) fewer predicted in *P. rubi* than in *P. fragariae* (**Table 5**).

357 **No distinguishing gene loss or gain; or the presence of INDELs or SNPs in candidate avirulence**

358 **genes could be found associated with race variation**

359 An orthology analysis of all predicted proteins from the isolates of *P. fragariae* and *P. rubi* assigned

360 481,942 (98.7%) proteins to 38,891 orthogroups. Of these groups, 17,101 contained at least one

361 protein from all fourteen sequenced isolates and 13,132 of these groups consisted entirely of single-

362 copy proteins from each isolate. There were 2,345 of these groups unique to *P. rubi* and 1,911 of these

363 groups unique to *P. fragariae*. Analysis of unique and expanded orthogroups for isolates of the UK1,

364 UK2 and UK3 races did not lead to the identification of candidate avirulence genes, as these groups

365 did not contain putative effector genes (**Figure 2**).

366 A total of 725,444 SNP sites and 95,478 small INDELs were identified within the *P. fragariae*

367 and *P. rubi* isolates by the Genome Analysis ToolKit (GATK) haplotypecaller (McKenna et al., 2010)

368 and 80,388 indels and 7,020 structural variants were identified by SvABA (Wala et al., 2018).

369 Analysis of high quality, biallelic SNP sites allowed the identification of a distinct population

370 consisting of the isolates of race UK1, UK2 and UK3, hereafter referred to as the UK1-2-3 population,

371 with SCRP245, the only UK isolate, potentially forming an ancestral or hybrid isolate between the

372 UK1-2-3 population and the population represented by BC-23 and ONT-3 (**Figure 3; Supplementary**

373 **Figure S2**). Additionally, clear separation between isolates of *P. fragariae* and *P. rubi* was observed.

374 Further analysis within the UK1-2-3 population allowed for the identification of private variants,

375 which were only present in isolates of one of the three races in this population. This resulted in the

376 identification of eleven private variants in the UK2 race shared between both A4 and BC-16; however,

377 neither the genes they fell within or were neighbours to were predicted to encode effectors or secreted

378 proteins and likely did not explain the differences in pathogenicity.

379 **Wide scale transcriptional reprogramming of effectors during strawberry infection**

380 RNA-Seq data were generated from an inoculation time course experiment for representatives of races

381 UK1, UK2 and UK3; BC-1, BC-16 and NOV-9 respectively. Following determination of expression

382 levels of the predicted genes in both *in planta* and mycelia samples, a correlation analysis showed

383 biological replicates of each timepoint grouped together (**Figure 4**). Additionally, the 48 hours post

384 inoculation (hpi) BC-1 time point grouped with the BC-16 24 hpi time point, suggesting these may

385 represent similar points in the infection process. However, clear separation between the BC-16

386 timepoints was observed (**Figure 4**). A total of 13,240 transcripts from BC-16 (32%) showed

387 expression above a FPKM value threshold of five in at least one sequenced BC-16 time point and

13

388   9,329 (23%) of these showed evidence of differential expression in at least one sequenced *in planta*
389   time point compared to mycelium grown in artificial media, suggesting large scale transcriptional
390   reprogramming. As three time points post inoculation were sequenced for BC-16, the changes in
391   expression over the course of the infection process was investigated. A total of 2,321 transcripts (6%)
392   showed a Log$_2$ Fold Change (LFC) greater than or equal to one or less than or equal to minus one,
393   representing a general reprofiling during infection in comparison to growth in artificial media. Of
394   transcripts differentially expressed *in planta* compared to artificial media, fewer transcripts were
395   differentially expressed at both 24 hpi and 96 hpi than between sequential timepoints (297 compared
396   to 1,016 and 1,604 transcripts). This suggested that changes during the progress of infection were
397   captured by this dataset (**Figure 5**).

398   Levels of expression of effector genes were also assessed. A total of 274 (26%) RxLR
399   effectors, 27 (31%) CRNs and 880 (18%) putative apoplastic effectors from BC-16 showed evidence
400   of expression above the FPKM threshold of 5 in at least one sequenced time point. The majority of
401   these effector genes also showed evidence of differential expression during *in planta* time points
402   compared to *in vitro* mycelium. A total of 253 (24%) RxLR effectors, 19 (22%) CRNs and 888 (18%)
403   putative apoplastic effectors showed an LFC greater than or equal to one or less than or equal to minus
404   one, representing wide scale transcriptional reprogramming of effector genes during infection (**Figure
405   5**). Ranking of the 50 highest expressed genes *in planta* with a LFC of ≥3 in comparison to its
406   respective mycelium, identified four putative RxLR genes that were upregulated by all three isolates
407   (**Table 6**). These genes represent putative core *P. fragariae* RxLR's important for pathogenicity on
408   strawberry. Interestingly, a BLASTP search of one of these putative core effectors, PF003_g16448
409   (amino acids 19-139), showed homology to *P. sojae Avr1b* (58 % pairwise identity), GenBank
410   accession AF449625 (Shan et al., 2004).

RxLR effector PF003_g27513 is a strong candidate for *PfAvr2*

412   Comparing transcripts with the highest LFC (*in planta* vs mycelium) between isolates led to the
413   identification of the putative RxLR effector encoding transcript PF003_g27513.t1 as a potential
414   candidate for *PfAvr2* in BC-16. PF003_g27513 had a peak FPKM value in BC-16 of 9,392 compared
415   to peaks of 5 and 34, in BC-1 and NOV-9, respectively (**Supplementary Table S2**). Subsequent RT-
416   qPCR analysis of further timepoints in the *in planta* timecourse supported the findings of the RNA-
417   Seq timepoints and showed the expression of putative *PfAvr2* in the UK2 isolates BC-16 and A4 was
418   significantly ($p < 0.05$) different to those from all samples of BC-1 (UK1) and NOV-9 (UK3; **Figure

14

419   **6**). A BLASTP search of PF003_g16448 (amino acids 26-137) revealed homology to *P. sojae*

420   *Avh6/Avr1d* (37 % pairwise identity), GenBank accession JN253642 (Wang et al., 2011; Na et al.,

421   2013).

422   The surrounding sequence of putative *PfAvr2* in BC-16, BC-1 and NOV-9 was investigated

423   for sequence variants that may explain the expression difference. As no variants were identified near

424   the gene from the above mentioned variant panel, an assembly of the NOV-9 isolate was created from

425   Nanopore sequencing data, producing an assembly of 93.72 Mbp in 124 contigs with an N50 of 1,260

426   Kb. This resulted in the identification of a SNP from T in BC-16 to G in NOV-9 ~14 Kb downstream

427   of the stop codon and a 30 bp insertion in NOV-9 ~19 Kb upstream of the start codon (**Figure 7A**).

428   The upstream variant appeared to be a sequencing error following the investigation of the alignment

429   of short reads of BC-16 and NOV-9 to each assembly and so was rejected. Expression of the genes

430   surrounding PF003_g27513 was investigated and PF003_g27514, directly upstream of putative

431   *PfAvr2* is expressed by all three isolates (**Supplementary Table S2**).

432   Additionally, putative transcription factors and transcriptional regulators were identified in all

433   sequenced genomes. This resulted in the identification of 269 genes in the BC-16 isolate of *P.*

434   *fragariae*. However, analysis of gene loss or gain and an investigation of variant sites showed no race

435   specific differences, though expression level variation was observed.

RxLR effector PF009_g26276 is a putative candidate for *PfAvr3*

437   Further analysis of the RNA-Seq datasets identified the putative RxLR effector encoding transcript

438   PF009_g26276 (an orthologue of PF003_g27386) as a potential candidate for *PfAvr3* in NOV-9, with

439   a peak FPKM value in NOV-9 of 199 compared to *in planta* peaks of 6 and 12 in BC-1 and BC-16,

440   respectively (**Supplementary Table S3**). Similar to putative *PfAvr2*, no sequence differences in

441   putative *PfAvr3* were observed between the three isolates. Analysis of the surrounding region between

442   NOV-9 and BC-16 showed no sequence differences 13,000 bp upstream and 3,761 bp downstream of

443   PF009_g26276 (**Figure 7B**). The two genes upstream from putative *PfAvr3* are not expressed in any

444   isolate (**Supplementary Table S3**), whereas the gene directly downstream in BC-16, PF003_g27385,

445   is expressed by all the three isolates analysed.

446   Subsequent RT-qPCR analysis of further timepoints in the *in planta* time course revealed that

447   the putative *PfAvr3* was not expressed during any timepoints by the UK1 isolate BC-1 or by the UK2

448   isolates BC-16 and A4 (**Supplementary Figure S3**). However, absolute expression of

15

449   PF009_g26276 in NOV-9 remained low. Expression in NOV-9 at 72 hpi was significantly ($p < 0.05$)

450   greater than those from all samples of BC-1, BC-16 and A4.

451   **Candidate genes for *PfAvr1* identified from expression level variation**

452   Analysis of the RNA-Seq datasets did not reveal an obvious candidate for *PfAvr1*. Further analysis

453   using custom scripts identified genes, which were uniquely expressed in BC-1 and those uniquely

454   differentially expressed. These genes were scored for confidence of race avirulence determinant; high,

455   medium and low. No genes were identified in the high confidence class in BC-1, but four genes were

456   scored as medium confidence, one of which was a putative apoplastic effector (**Supporting**

457   **Candidate Table**). The analysis was repeated for BC-16 and NOV-9, in case the putative RxLR

458   candidates are not *PfAvr*2 and *PfAvr3*, respectively (**Supporting Candidate Table**).

459

460   **DISCUSSION**

461   Understanding pathogenicity of plant pathogens is critical for developing durable resistance strategies.

462   *P. fragariae* is a continuing threat to strawberry production. The UK1-2-3 population displayed clear

463   separation from the other isolates of *P. fragariae* in this study. Two putative avirulence candidates for

464   UK2 and UK3 were identified through population resequencing and analyses of gene expression

465   during *P. fragariae* infection. We have shown that there are no distinguishing gene loss or gain events,

466   INDELs or SNPs associated with race variation in UK1-2-3. Our results also suggest that the

467   polymorphisms associated with avirulence to race UK2 and UK3 resistance is controlled *in trans* or

468   with other stable forms of epigenetic modulating gene expression.

469   This study utilised long read sequencing technologies to improve the contiguity of the *P.*

470   *fragariae* genome through the assembly of a greater amount of repeat rich sequence. Though this

471   assembly still fell short of the estimated chromosome number of 10 - 12 (Brasier et al., 1999), at 180

472   contigs, it is a significant improvement over the previous assemblies that utilised solely short read

473   technologies and produced relatively fragmented assemblies, comprised of >1,000 contigs each (Gao

474   et al., 2015; Tabima et al., 2017). The increase in size of the assembly presented (91 Mb), suggests

475   that the assembly includes an increased amount of repetitive sequence, indicating that it represents a

476   more complete genome assembly than previous attempts. Although the assembly presented here was

477   larger than previously reported assemblies, it is similar in size to the related Clade 7b species *P. sojae*

478   (95 Mb; Tyler et al., 2006). This study produced assemblies of an additional ten isolates of *P. fragariae*

479   and three isolates of the closely related raspberry pathogen *P. rubi* with short read technology. These

16

480   assemblies were of similar sizes and contiguity to those previously published (Gao et al., 2015;

481   Tabima et al., 2017).

482   All assemblies produced from PacBio and Illumina sequencing were annotated and putative

483   effector genes were predicted. The gene model totals are likely inflated, due to the use of a greedy

484   approach to effector gene prediction, to ensure the capture of all possible virulence genes. ApoplastP

485   appeared to over-predict effectors, likely due to statistical issues arising from the use of a training set

486   far smaller than the query set used in this study (Pritchard and Broadhurst, 2014). Interestingly, twice

487   as many CRNs were predicted in *P. rubi* than *P. fragariae* on average (average of 118 in *P. rubi* and

488   67 in *P. fragariae*), though this was not consistent for all *P. rubi* isolates. In comparison to *P. sojae*,

489   the BC-16 isolate was predicted to possess approximately 50% more RxLRs and twice as many CRNs

490   from RNA-Seq guided gene models (Tyler et al., 2006). This difference may have been due to

491   improvements in prediction strategies, as the number of CRNs was similar to those predicted for the

492   Clade 1 species *P. cactorum* (Armitage et al., 2018). However for RxLR effectors this difference is

493   likely explained by the greedy approach taken for gene prediction in this study. Following the

494   validation of gene models by RNA-Seq data, the likely overprediction of effector genes was also

495   shown by the low percentage of these classes of genes showing evidence of expression.

496   This work also allowed the resolution of *P. fragariae* race schemes between different

497   countries, Canadian race 1 is equivalent to UK race 1, Canadian race 2 is equivalent to UK race 3 and

498   both Canadian race 3 and USA race 4 is equivalent to UK race 2. This provided further support for

499   the proposed gene-for-gene model of resistance in this pathosystem (van de Weg, 1997a). However,

500   construction of orthology groups for all isolates of *P. fragariae* and *P. rubi* did not show the presence

501   of proteins unique to the races UK1, UK2 and UK3. Additionally, the identification of variant sites,

502   with the BC-16 genome acting as a reference, indicated there were only private variants present in

503   UK2, with none identified in UK1 or UK3. None of these variants were in proximity to genes thought

504   to be involved in pathogenicity. Additionally, analysis of population structure confirmed the

505   previously described species separation of *P. fragariae* and *P. rubi* (Man in 't Veld, 2007; Tabima et

506   al., 2018) and identified a subpopulation consisting of the isolates of *P. fragariae* of UK1-2-3 on

507   which further investigations focused.

508   Transcriptome analyses led to the identification of a strong candidate for *PfAvr2*, which was

509   shown to be highly expressed in all *in planta* BC-16 timepoints, compared to evidence of no, or very

510   low levels of expression in any BC-1 (UK1) or NOV-9 (UK3) samples. The strongest candidate for

511   *PfAvr3* was also shown to be differentially expressed between races, but not as highly expressed in

17

512   NOV-9 as observed for putative *PfAvr2*. RT-qPCR confirmed the *PfAvr2* results and additionally

513   showed expression of *PfAvr2* in the other sequenced UK2 isolate, A4. The assay showed high levels

514   of variability, which was due to variation between biological replicates, likely the result of the inability

515   of the inoculation method to control the quantity of zoospores inoculating an individual plant. Further

516   *in planta* experiments and RT-qPCR of additional isolates are required to investigate the observations

517   of putative *PfAvr3*.

518   We propose that silencing of putative *PfAvr2* in races UK1 and UK3, enables those isolates to

519   evade recognition in *Rpf2* possessing plants, such as 'Redgauntlet', but not in plants possessing '*Rpf1*'

520   or '*Rpf3*', respectively. Silencing of putative *PfAvr3* also enables races UK1 and UK2 to evade

521   recognition in *Rpf3* possessing plants, as long as they also do not possess *Rpf1* and *Rpf3*.

522   Whilst the exact mechanism of putative *PfAvr2* and *PfAvr3* silencing was not identified in this

523   study, long read sequencing of a race UK3 isolate (NOV-9) identified a single SNP, 14 kb downstream

524   of the stop codon of putative *PfAvr2* and variation in expression of transcription factors was observed

525   in the RNA-Seq data. This indicated that epigenetic modifications could explain the observed

526   transcriptional variation. Transcriptional silencing of effectors is a known mechanism that

527   *Phytophthora* spp. employ to evade the activation of host *R*-gene-mediated immunity. Investigations

528   of the EC-1 clonal lineage of *P. infestans* revealed a variation of the ability of isolates to cause disease

529   on potato plants possessing the *Rpi-vnt1.1* gene. It was shown, in the absence of genetic mutations,

530   that differences in the expression level of *Avrvnt1* were detected that correlated with virulence (Pais

531   et al., 2018). Recent work in *P. infestans* and *P. sojae* has shown evidence of adenine N6-methylation

532   (6mA) alongside a lack of evidence of 5-methylcytosine (5mC) DNA methylation, highlighting that

533   6mA methylation is an important epigenetic mark for the regulation of gene expression in

534   *Phytophthora* spp. (Chen et al., 2018). It is also possible that chromatin modifications may be involved

535   in controlling the expression differences, as demonstrated in *P. infestans* (van West et al., 2008; Chen

536   et al., 2018). Investigation of these possibilities, while not achievable in the current study is a clear

537   direction for future research.

538   Nearly all *P. fragariae* isolates investigated in this study were collected from around Canada

539   between 2001-2012. The SCRP245 isolate was identified as an intermediate between the UK1-2-3

540   population and the population represented by the BC-23 and ONT-3 isolates. SCRP245 could

541   represent a rare hybrid of the two populations. However, due to the small sample size of isolates, the

542   low number of SNP sites available for this analysis and the fact it was isolated in 1945 in the UK, at

543   least 55 years before the other isolates, it appears more likely that SCRP245 represents a separate

544 population but the data available were unable to resolve this fully. Further race typing with differential

545 strawberry genotypes is required to ascertain the relationship between isolates of Canadian races 4

546 and 5.

547   Races of asexual species have been shown to evolve by the stepwise accumulation of

548 mutations (Del Mar Jiménez-Gasco et al., 2004). One such example is the successive evolution of

549 multiple pathotypes in a single clonal lineage of the wheat pathogen *Puccinia striiformis* f. sp. *tritici*

550 in Australia and New Zealand (Steele et al., 2001). In comparison, our data do not indicate that *P.*

551 *fragariae* has undergone simple stepwise evolution of effectors, but we rather postulate that some

552 lineages of *P. fragariae* have been present for long periods of time in nature, evident by the large

553 number of SNP differences and well supported branches and that the emergence of races (e.g. UK1-

554 2-3) is fairly recent, possibly as a result of the *R*-genes deployed in commercial strawberries. The

555 increased selection pressure on *P. fragariae* to overcome these genes, or the break-up of 'wild' *R*-

556 gene stacks upon hybridisation of octoploid strawberry species, may have led to very rapid evolution

557 of races, in this case through epigenetic silencing of gene expression, to evade the *R*-genes present in

558 common cultivars. Substantial further sampling from multiple geographic regions would be required

559 to fully decipher population structure in the lineages of *P. fragariae* and the resistance status of wild

560 octoploid *Fragaria* species. We predict that this would lead to the observation of other geographically

561 distinct lineages of genetically similar individuals of *P. fragariae* but with similar differences in

562 pathogenicity on strawberry. The implications of these findings highlight the potential adaptability of

563 *P. fragariae* to modify effector expression to evade host resistance and the threat of the emergence of

564 new races. Future strawberry breeding efforts must deploy cultivars with multiple resistance genes to

565 mitigate against the rapid adaptation of *P. fragariae*. Identifying resistance genes that recognise the

566 conserved core RxLRs identified in this study would enable broad-spectrum resistance to this

567 pathogen to be deployed that would be effective against multiple races. One of the conserved highly

568 expressed RxLRs was shown to have homology to *P. sojae Avr1b* and so identifying homologous *R*-

569 genes to *Rsp1b* in strawberry could be a future avenue of work to provide resistance against multiple

570 races.

571   In conclusion, we have shown for the first time that within a distinct subpopulation of *P.*

572 *fragariae* isolates, displaying remarkably low levels of polymorphisms, the ability to cause disease on

573 a range of differing strawberry cultivars was associated with variation in transcriptional levels rather

574 than being due to sequence variation, similar to reports in *P. infestans* (Pais et al., 2018). This work

575 therefore has implications for the identification of putative avirulence genes in the absence of

576 associated expression data and highlights the need for detailed molecular characterisation of
577 mechanisms of effector regulation and silencing in oomycete plant pathogens. In addition, this study
578 presents a large amount of data, including an improved, long read assembly of *P. fragariae* alongside
579 a collection of resequenced isolates of *P. fragariae* and *P. rubi*, and transcriptome data from multiple
580 isolates that is a valuable resource for future studies.

581

AUTHOR CONTRIBUTIONS

583 RH, CN and TA devised the study. RH, CN and JD co-supervised TA's PhD study, within which
584 some of this work was undertaken. TA performed the experimental work, with contributions from
585 CN. AA assisted with the development of genome assembly, annotation and orthology pipelines. MS
586 developed elements of the variant calling pipeline and structure analysis with TA. HB performed
587 Nanopore and MiSeq sequencing. JT, BK, BT and NG provided RNA-Seq reads of *P. rubi* for genome
588 annotation. TA drafted the manuscript with input from CN, JD and RH. All authors read and approved
589 the submission.

590

595

605

606

20

DATA AVAILABILITY STATEMENT

607

608   The datasets, including all assemblies and annotations, generated for this study are available on NCBI

609   GenBank as part of BioProjects PRJNA396163 and PRJNA488213 with accession numbers of

610   SAMN07449679 - SAMN07449692. Raw sequencing reads have been deposited in the NCBI SRA,

611   DNA-Seq reads are available with accession codes SRR7668085 - SRR7668100 and *P. fragariae*

612   RNA-Seq reads are available with accession codes SRR7764607 - SRR7764615. *P. rubi* RNA-Seq

613   reads are available with the accession codes SRR10207404 - SRR10207405.

REFERENCES

614

615 Adams, T. M. (2019). Pathogenomics of *Phytophthora fragariae*, the causal agent of strawberry red
616   core disease [PhD thesis]. [Reading (UK)]: University of Reading.

617 Altschul, S. F., Madden, T. L., Schäffer, A. A., Zhang, J., Zhang, Z., Miller, W., and Lipman, D. J.
618   (1997). Gapped BLAST and PSI-BLAST: a new generation of protein database search
619   programs. *Nucleic Acids Res*. 25, 3389-3402.

620 Armenteros, J. J. A., Tsirigos, K. D., Sønderby, C. K., Petersen, T. N., Winther, O., Brunak, S., et al.
621   (2019). SignalP 5.0 improves signal peptide predictions using deep neural networks. *Nat.
622   Biotechnol.* 37, 420–423. doi.org/10.1038/s41587-019-0036-z.

623 Armitage, A. D., Lysøe, E., Nellist, C. F., Lewis, L. A., Cano, L. M., Harrison, R. J., et al. (2018).
624   Bioinformatic characterisation of the effector repertoire of the strawberry pathogen
625   *Phytophthora cactorum*. *PLoS ONE* 13, e0202305. doi:10.1371/journal.pone.0202305.

626 Aronesty, E. (2013). Comparison of Sequencing Utility Programs. *Open Bioinforma. J.* 7, 1–8.
627   doi:10.2174/1875036201307010001.

628 Bankevich, A., Nurk, S., Antipov, D., Gurevich, A. A., Dvorkin, M., Kulikov, A. S., et al. (2012).
629   SPAdes: a new genome assembly algorithm and its applications to single-cell sequencing. *J.
630   Comput. Biol.* 19, 455–477. doi:10.1089/cmb.2012.0021.

631 Bendtsen, J. D., Nielsen, H., von Heijne, G. and Brunak, S. (2004) Improved Prediction of Signal
632   Peptides: SignalP 3.0. *J. Mol. Biol*. **340**(4), 783-795. doi:10.1016/j.jmb.2004.05.028.

633 Brasier, C. M., Cooke, D. E., and Duncan, J. M. (1999). Origin of a new Phytophthora pathogen
634   through interspecific hybridization. *Proc Natl Acad Sci USA* 96, 5878–5883.
635   doi:10.1073/pnas.96.10.5878.

636 Buitrago-Flórez, F. J., Restrepo, S., and Riaño-Pachón, D. M. (2014). Identification of transcription
637   factor genes and their correlation with the high diversity of stramenopiles. *PLoS ONE* 9,
638   e111841. doi:10.1371/journal.pone.0111841.

639 Campbell, A. M., Moon, R. P., Duncan, J. M., Gurr, S.-J., and Kinghorn, J. R. (1989). Protoplast
640   formation and regeneration from sporangia and encysted zoospores of *Phytophthora infestans*.
641   *Physiol. Mol. Plant P.* 34, 299–307. doi:10.1016/0885-5765(89)90027-1.

642 Clifford, R. J., Milillo, M., Prestwood, J., Quintero, R., Zurawski, D. V., Kwak, Y. I., et al. (2012)
643   Detection of Bacterial 16S rRNA and Identification of Four Clinically Important Bacteria by
644   Real-Time PCR. *PLoS ONE* 7, e48558. doi:10.1371/journal.pone.0048558

645 Chen, H., and Boutros, P. C. (2011). VennDiagram: a package for the generation of highly-
646   customizable Venn and Euler diagrams in R. *BMC Bioinformatics* 12, 35. doi:10.1186/1471-
647   2105-12-35.

648 Chen, H., Shu, H., Wang, L., Zhang, F., Li, X., Ochola, S. O., et al. (2018). Phytophthora
649   methylomes are modulated by 6mA methyltransferases and associated with adaptive genome
650   regions. *Genome Biol.* 19, 181. doi:10.1186/s13059-018-1564-4.

651 Chin, C.-S., Alexander, D. H., Marks, P., Klammer, A. A., Drake, J., Heiner, C., et al. (2013).
652   Nonhybrid, finished microbial genome assemblies from long-read SMRT sequencing data. *Nat.
653   Methods* 10, 563–569. doi:10.1038/nmeth.2474.

22

654   Chin, C.-S., Peluso, P., Sedlazeck, F. J., Nattestad, M., Concepcion, G. T., Clum, A., et al. (2016).
655   Phased diploid genome assembly with single-molecule real-time sequencing. *Nat. Methods* 13,
656   1050–1054. doi:10.1038/nmeth.4035.

657   Cui, C., Herlihy, J., Bombarely, A., McDowell, J. M., and Haak, D. C. (2019). Draft assembly of
658   *Phytopthora capsici* from long-read sequencing uncovers complexity. *Mol. Plant Microbe
659   Interact.* doi:10.1094/MPMI-04-19-0103-TA.

660   Danecek, P., Auton, A., Abecasis, G., Albers, C. A., Banks, E., DePristo, M. A., et al. (2011). The
661   variant call format and VCFtools. *Bioinformatics* 27, 2156–2158.
662   doi:10.1093/bioinformatics/btr330.

663   Del Mar Jiménez-Gasco, M., Milgroom, M. G., and Jiménez-Díaz, R. M. (2004). Stepwise Evolution
664   of Races in *Fusarium oxysporum* f. sp. *ciceris* Inferred from Fingerprinting with Repetitive
665   DNA Sequences. *Phytopathology* 94, 228–235. doi:10.1094/PHYTO.2004.94.3.228.

666   Dobin, A., Davis, C. A., Schlesinger, F., Drenkow, J., Zaleski, C., Jha, S., et al. (2013). STAR:
667   ultrafast universal RNA-seq aligner. *Bioinformatics* 29, 15–21.
668   doi:10.1093/bioinformatics/bts635.

669   Dong, S., Qutob, D., Tedman-Jones, J., Kuflu, K., Wang, Y., Tyler, B. M., et al. (2009). The
670   *Phytophthora sojae* avirulence locus Avr3c encodes a multi-copy RXLR effector with sequence
671   polymorphisms among pathogen strains. *PLoS ONE* 4, e5556.
672   doi:10.1371/journal.pone.0005556.

673   EFSA Panel on Plant Health (PLH) (2014). Scientific Opinion on the risks to plant health posed by
674   *Phytophthora fragariae* Hickman var. *fragariae* in the EU territory, with the identification and
675   evaluation of risk reduction options. *EFSA Journal* 12. doi:10.2903/j.efsa.2014.3539.

676   Emms, D. M., and Kelly, S. (2015). OrthoFinder: solving fundamental biases in whole genome
677   comparisons dramatically improves orthogroup inference accuracy. *Genome Biol.* 16, 157.
678   doi:10.1186/s13059-015-0721-2.

679   EPPO (2018). EPPO A2 List. *EPPO A2 List*. Available at:
680   https://www.eppo.int/ACTIVITIES/plant_quarantine/A2_list [Accessed January 31, 2019].

681   Gao, R., Cheng, Y., Wang, Y., Wang, Y., Guo, L., and Zhang, G. (2015). Genome Sequence of
682   *Phytophthora fragariae* var. *fragariae*, a Quarantine Plant-Pathogenic Fungus. *Genome
683   Announc.* 3. doi:10.1128/genomeA.00034-15.

684   Garrison, E. (2012). *Vcflib. A C++ library for parsing and manipulating VCF files*. Github
685   Available at: https://github.com/ekg/vcflib [Accessed December 19, 2018].

686   Gurevich, A., Saveliev, V., Vyahhi, N., and Tesler, G. (2013). QUAST: quality assessment tool for
687   genome assemblies. *Bioinformatics* 29, 1072–1075. doi:10.1093/bioinformatics/btt086.

688   Haas, B. (2010). *TransposonPSI: an application of PSI-blast to mine (Retro-)transposon ORF
689   homologies*. sourceforge Available at: http://transposonpsi.sourceforge.net/ [Accessed January
690   10, 2019].

691   Hickman, C. J. (1941). The Red Core Root Disease of The Strawberry Caused By *Phytophthora
692   Fragariae* n.sp. *Journal of Pomology and Horticultural Science* 18, 89–118.
693   doi:10.1080/03683621.1941.11513556.

694 Hoff, K. J., Lange, S., Lomsadze, A., Borodovsky, M., and Stanke, M. (2016). BRAKER1:
695   Unsupervised RNA-Seq-Based Genome Annotation with GeneMark-ET and AUGUSTUS.
696   *Bioinformatics* 32, 767–769. doi:10.1093/bioinformatics/btv661.

697 Judelson, H. S., Coffey, M. D., Arredondo, F. R., and Tyler, B. M. (1993). Transformation of the
698   oomycete pathogen *Phytophthora megasperma* f. sp. *glycinea* occurs by DNA integration into
699   single or multiple chromosomes. *Curr. Genet.* 23, 211–218. doi:10.1007/BF00351498.

700 Käll L., Krogh, A. and Sonnhammer, E. L. L. (2004). A Combined Transmembrane Topology and
701   Signal Peptide Prediction Method. *J. Mol. Biol.* 338(5), 1027-1036.
702   doi:10.1016/j.jmb.2004.03.016.

703 Katoh, K., Misawa, K., Kuma, K., and Miyata, T. (2002). MAFFT: a novel method for rapid
704   multiple sequence alignment based on fast Fourier transform. *Nucleic Acids Res.* 30, 3059–
705   3066. doi:10.1093/nar/gkf436.

706 Katoh, K., and Standley, D. M. (2013). MAFFT multiple sequence alignment software version 7:
707   improvements in performance and usability. *Mol. Biol. Evol.* 30, 772–780.
708   doi:10.1093/molbev/mst010.

709 Koren, S., Walenz, B. P., Berlin, K., Miller, J. R., Bergman, N. H., and Phillippy, A. M. (2017).
710   Canu: scalable and accurate long-read assembly via adaptive k-mer weighting and repeat
711   separation. *Genome Res.* 27, 722–736. doi:10.1101/gr.215087.116.

712 Langmead, B., and Salzberg, S. L. (2012). Fast gapped-read alignment with Bowtie 2. *Nat. Methods*
713   9, 357–359. doi:10.1038/nmeth.1923.

714 Liao, Y., Smyth, G. K., and Shi, W. (2014). featureCounts: an efficient general purpose program for
715   assigning sequence reads to genomic features. *Bioinformatics* 30, 923–930.
716   doi:10.1093/bioinformatics/btt656.

717 Livak, K. J., and Schmittgen, T. D. (2001). Analysis of relative gene expression data using real-time
718   quantitative PCR and the 2(-Delta Delta C(T)) Method. *Methods* 25, 402–408.
719   doi:10.1006/meth.2001.1262.

720 Li, H. (2013). Aligning sequence reads, clone sequences and assembly contigs with BWA-MEM.
721   *arXiv*.

722 Li, H. (2018). Minimap2: pairwise alignment for nucleotide sequences. *Bioinformatics* 34, 3094–
723   3100. doi:10.1093/bioinformatics/bty191.

724 Li, H., Handsaker, B., Wysoker, A., Fennell, T., Ruan, J., Homer, et al. (2009). The Sequence
725   Alignment/Map format and SAMtools. *Bioinformatics* 25, 2078–2079.
726   doi:10.1093/bioinformatics/btp352.

727 Love, M. I., Huber, W., and Anders, S. (2014). Moderated estimation of fold change and dispersion
728   for RNA-seq data with DESeq2. *Genome Biol.* 15, 550. doi:10.1186/s13059-014-0550-8.

729 Maas, J. L. (1972). Growth and reproduction in culture of ten *Phytophthora fragariae* races.
730   *Mycopathol. Mycol. Appl.* 48, 323–334. doi:10.1007/BF02052636.

731 Malar C, M., Yuzon, J. D., Das, S., Das, A., Panda, A., Ghosh, S., et al. (2019). Haplotype-Phased
732   Genome Assembly of Virulent *Phytophthora ramorum* Isolate ND886 Facilitated by Long-
733   Read Sequencing Reveals Effector Polymorphisms and Copy Number Variation. *Mol. Plant*
734   *Microbe Interact.* 32, 1047–1060. doi:10.1094/MPMI-08-18-0222-R.

24

735 Man in 't Veld, W. A. (2007). Gene flow analysis demonstrates that *Phytophthora fragariae* var.*rubi*
736   constitutes a distinct species, *Phytophthora rubi* comb. nov. *Mycologia* 99, 222–226.
737   doi:10.1080/15572536.2007.11832581.

738 McKenna, A., Hanna, M., Banks, E., Sivachenko, A., Cibulskis, K., Kernytsky, A., et al. (2010). The
739   Genome Analysis Toolkit: a MapReduce framework for analyzing next-generation DNA
740   sequencing data. *Genome Res.* 20, 1297–1303. doi:10.1101/gr.107524.110.

741 Na, R., Yu, D., Qutob, D., Zhao, J., and Gijzen, M. (2013). Deletion of the *Phytophthora sojae*
742   avirulence gene *Avr1d* causes gain of virulence on *Rsp1d*. *Mol. Plant Microbe Interact.* 26(6),
743   969–976. doi.org/10.1094/MPMI-02-13-0036-R.

744 Nielsen, H., Englebrecht, J., Brunak S. and von Heijne G. (1997). Identification of prokaryotic and
745   eukaryotic signal peptides and prediction of their cleavage sites. *Protein Eng.* 10(1), 1-6.
746   doi:10.1093/protein/10.1.1.

747 Pais, M., Yoshida, K., Giannakopoulou, A., Pel, M. A., Cano, L. M., Oliva, R. F., et al. (2018). Gene
748   expression polymorphism underpins evasion of host immunity in an asexual lineage of the Irish
749   potato famine pathogen. *BMC Evol. Biol.* 18, 93. doi:10.1186/s12862-018-1201-6.

750 Petersen, T. N., Brunak, S., Heijne, von, G., & Nielsen, H. (2011). SignalP 4.0: discriminating signal
751   peptides from transmembrane regions. *Nat. Methods*, 8, 785–786. doi:10.1038/nmeth.1701.

752 van Poppel, P. M. J. A., Guo, J., van de Vondervoort, P. J. I., Jung, M. W. M., Birch, P. R. J.,
753   Whisson, S. C., et al. (2008). The *Phytophthora infestans* avirulence gene Avr4 encodes an
754   RXLR-dEER effector. *Mol. Plant Microbe Interact.* 21, 1460–1470. doi:10.1094/MPMI-21-11-
755   1460.

756 Pritchard, L., and Broadhurst, D. (2014). On the statistics of identifying candidate pathogen
757   effectors. *Methods Mol. Biol.* 1127, 53–64. doi:10.1007/978-1-62703-986-4_4.

758 Purcell, S., Neale, B., Todd-Brown, K., Thomas, L., Ferreira, M. A. R., Bender, D., et al. (2007).
759   PLINK: a tool set for whole-genome association and population-based linkage analyses. *Am. J.*
760   *Hum. Genet.* 81, 559–575. doi:10.1086/519795.

761 Raj, A., Stephens, M., and Pritchard, J. K. (2014). fastSTRUCTURE: variational inference of
762   population structure in large SNP data sets. *Genetics* 197, 573–589.
763   doi:10.1534/genetics.114.164350.

764 Robinson Boyer, L., Feng, W., Gulbis, N., Hajdu, K., Harrison, R. J., Jeffries, P., et al. (2016). The
765   use of arbuscular mycorrhizal fungi to improve strawberry production in coir substrate. *Front.*
766   *Plant. Sci.* 7, 1237. doi:10.3389/fpls.2016.01237.

767 Ruan, J. (2018). *SMARTdenovo: Ultra-fast de novo assembler using long noisy reads.* Github
768   Available at: https://github.com/ruanjue/smartdenovo [Accessed January 10, 2019].

769 R Core Team (2016). *R: A Language and Environment for Statistical Computing.* R Foundation for
770   Statistical Computing, Vienna, Austria Available at: https://www.R-project.org [Accessed
771   December 19, 2018].

772 R core team (2017). *R: A language and environment for statistical computing.* R Foundation for
773   Statistical Computing, Vienna, Austria Available at: https://www.R-project.org [Accessed
774   December 19, 2018].

775   Shan, W., Cao, M., Leung, D., & Tyler, B. M. (2004). The *Avr1b* locus of *Phytophthora sojae*
776   encodes an elicitor and a regulator required for avirulence on soybean plants carrying resistance
777   gene *Rps1b*. *Mol. Plant Microbe Interact.* 17(4), 394–403. doi: 10.1094/MPMI.2004.17.4.394.

778   Shulaev, V., Sargent, D. J., Crowhurst, R. N., Mockler, T. C., Folkerts, O., Delcher, et al. (2011).
779   The genome of woodland strawberry (*Fragaria vesca*). *Nat. Genet.* 43, 109–116.
780   doi:10.1038/ng.740.

781   Simão, F. A., Waterhouse, R. M., Ioannidis, P., Kriventseva, E. V., and Zdobnov, E. M. (2015).
782   BUSCO: assessing genome assembly and annotation completeness with single-copy orthologs.
783   *Bioinformatics* 31, 3210–3212. doi:10.1093/bioinformatics/btv351.

784   Simpson, J. (2018). *Nanopolish: Signal-level algorithms for MinION data*. Github Available at:
785   https://github.com/jts/nanopolish [Accessed January 10, 2019].

786   Smit, A. F. A., and Hubley, R. (2015). *RepeatModeler Open-1.0*. Repeatmasker.org Available at:
787   http://www.repeatmasker.org [Accessed January 10, 2019].

788   Smit, A. F. A., Hubley, R., and Green, P. (2015). *RepeatMasker Open-4.0*. repeatmasker.org
789   Available at: http://www.repeatmasker.org [Accessed January 10, 2019].

790   Sperschneider, J., Dodds, P. N., Singh, K. B., and Taylor, J. M. (2018). ApoplastP: prediction of
791   effectors and plant proteins in the apoplast using machine learning. *New Phytol.* 217, 1764–
792   1778. doi:10.1111/nph.14946.

793   Steele, K. A., Humphreys, E., Wellings, C. R., and Dickinson, M. J. (2001). Support for a stepwise
794   mutation model for pathogen evolution in Australasian *Puccinia striiformis* f.sp. *tritici* by use of
795   molecular markers. *Plant Pathology* 50, 174–180. doi:10.1046/j.1365-3059.2001.00558.x.

796   Tabima, J. F., Coffey, M. D., Zazada, I. A., and Grünwald, N. J. (2018). Populations of
797   *Phytophthora rubi* Show Little Differentiation and High Rates of Migration Among States in
798   the Western United States. *Mol. Plant Microbe Interact.* 31, 614–622. doi:10.1094/MPMI-10-
799   17-0258-R.

800   Tabima, J. F., Kronmiller, B. A., Press, C. M., Tyler, B. M., Zasada, I. A., and Grünwald, N. J.
801   (2017). Whole Genome Sequences of the Raspberry and Strawberry Pathogens *Phytophthora*
802   *rubi* and *P. fragariae*. *Mol. Plant Microbe Interact.* 30, 767–769. doi:10.1094/MPMI-04-17-
803   0081-A.

804   Taylor, A., Vágány, V., Jackson, A. C., Harrison, R. J., Rainoni, A., and Clarkson, J. P. (2016).
805   Identification of pathogenicity-related genes in *Fusarium oxysporum* f. sp. *cepae*. *Mol. Plant*
806   *Pathol.* 17, 1032–1047. doi:10.1111/mpp.12346.

807   Testa, A. C., Hane, J. K., Ellwood, S. R., and Oliver, R. P. (2015). CodingQuarry: highly accurate
808   hidden Markov model gene prediction in fungal genomes using RNA-seq transcripts. *BMC*
809   *Genomics* 16, 170. doi:10.1186/s12864-015-1344-4.

810   Thorvaldsdóttir, H., Robinson, J. T., and Mesirov, J. P. (2013). Integrative Genomics Viewer (IGV):
811   high-performance genomics data visualization and exploration. *Brief. Bioinformatics* 14, 178–
812   192. doi:10.1093/bib/bbs017.

813   Tyler, B. M., Tripathy, S., Zhang, X., Dehal, P., Jiang, R. H. Y., Aerts, A., et al. (2006).
814   Phytophthora genome sequences uncover evolutionary origins and mechanisms of pathogenesis.
815   *Science* 313, 1261–1266. doi:10.1126/science.1128796.

816 Untergasser, A., Cutcutache, I., Koressaar, T., Ye, J., Faircloth, B. C., Remm, M., et al. (2012).
817   Primer3--new capabilities and interfaces. *Nucleic Acids Res.* 40, e115. doi:10.1093/nar/gks596.

818 Vaser, R., Sović, I., Nagarajan, N., and Šikić, M. (2017). Fast and accurate de novo genome
819   assembly from long uncorrected reads. *Genome Res.* 27, 737–746. doi:10.1101/gr.214270.116.

820 Wala, J. A., Bandopadhayay, P., Greenwald, N. F., O'Rourke, R., Sharpe, T., Stewart, C., et al.
821   (2018). SvABA: genome-wide detection of structural variants and indels by local assembly.
822   *Genome Res.* 28, 581–591. doi:10.1101/gr.221028.117.

823 Walker, B. J., Abeel, T., Shea, T., Priest, M., Abouelliel, A., Sakthikumar, S., et al. (2014). Pilon: an
824   integrated tool for comprehensive microbial variant detection and genome assembly
825   improvement. *PLoS ONE* 9, e112963. doi:10.1371/journal.pone.0112963.

826 van de Weg, W. E. (1997a). A gene-for-gene model to explain interactions between cultivars of
827   strawberry and races of *Phytophthora fragariae* var. *fragariae. Theor. Appl. Genet.* 94, 445–
828   451. doi:10.1007/s001220050435.

829 van de Weg, W. E. (1997b). *Gene-for-gene relationships between strawberry and the causal agent of
830   red stele root rot,* Phytophthora fragariae *var.* fragariae.

831 van de Weg, W. E., Giezen, S., Henken, B., and den Nijs, A. P. M. (1996). A quantitative
832   classification method for assessing resistance to *Phytophthora fragariae* var. *fragariae* in
833   strawberry. *Euphytica* 91, 119–125. doi:10.1007/BF00035282.

834 van West, P., Shepherd, S. J., Walker, C. A., Li, S., Appiah, A. A., Grenville-Briggs, L. J., et al.
835   (2008). Internuclear gene silencing in *Phytophthora infestans* is established through chromatin
836   remodelling. *Microbiology* 154, 1482–1490. doi:10.1099/mic.0.2007/015545-0.

837 Wang, Q., Han, C., Ferreira, A. O., Yu, X., Ye, W., Tripathy, S., et al. (2011). Transcriptional
838   programming and functional interactions within the *Phytophthora sojae* RXLR effector
839   repertoire. *The Plant Cell.* 23(6), 2064–2086. doi.org/10.1105/tpc.111.086082.

840 Whisson, S. C., Boevink, P. C., Moleleki, L., Avrova, A. O., Morales, J. G., Gilroy, E. M., et al.
841   (2007). A translocation signal for delivery of oomycete effector proteins into host plant cells.
842   *Nature.* 450(7166), 115-118. doi:10.1038/nature06203.

843 Wickham, H. (2016). *ggplot2: Elegant Graphics for Data Analysis.* 2nd, illustrated ed. Springer.

844 Wick, R. (2018). *Porechop: adapter trimmer for Oxford Nanopore reads.* Github Available at:
845   https://github.com/rrwick/Porechop [Accessed January 9, 2019].

846 Wilcox, W. F., Scott, P. H., Hamm, P. B., Kennedy, D. M., Duncan, J. M., Brasier, C. M., et al.
847   (1993). Identity of a Phytophthora species attacking raspberry in Europe and North America.
848   *Mycol. Res.* 97, 817–831. doi:10.1016/S0953-7562(09)81157-X.

849 Yan, H.-Z., and Liou, R.-F. (2006). Selection of internal control genes for real-time quantitative RT-
850   PCR assays in the oomycete plant pathogen *Phytophthora parasitica. Fungal Genet. Biol.* 43,
851   430–438. doi:10.1016/j.fgb.2006.01.010.

852 Yin, W., Dong, S., Zhai, L., Lin, Y., Zheng, X., and Wang, Y. (2013). The *Phytophthora sojae*
853   Avr1d gene encodes an RxLR-dEER effector with presence and absence polymorphisms among
854   pathogen strains. *Mol. Plant Microbe Interact.* 26, 958–968. doi:10.1094/MPMI-02-13-0035-R.

855   Yu, D., Tang, H., Zhang, Y., Du, Z., Yu, H., and Chen, Q. (2012). Comparison and Improvement of
856   Different Methods of RNA Isolation from Strawberry (*Fragaria × ananassa*). *JAS* 4.
857   doi:10.5539/jas.v4n7p51.

858

859   **Conflict of Interest Statement:** The authors declare that the research was conducted in the absence

860   of any commercial or financial relationships that could be constructed as a potential conflict of
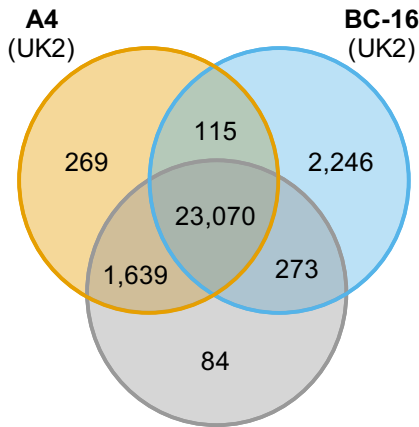
861   interest.

862

863

864

865   **FIGURES**
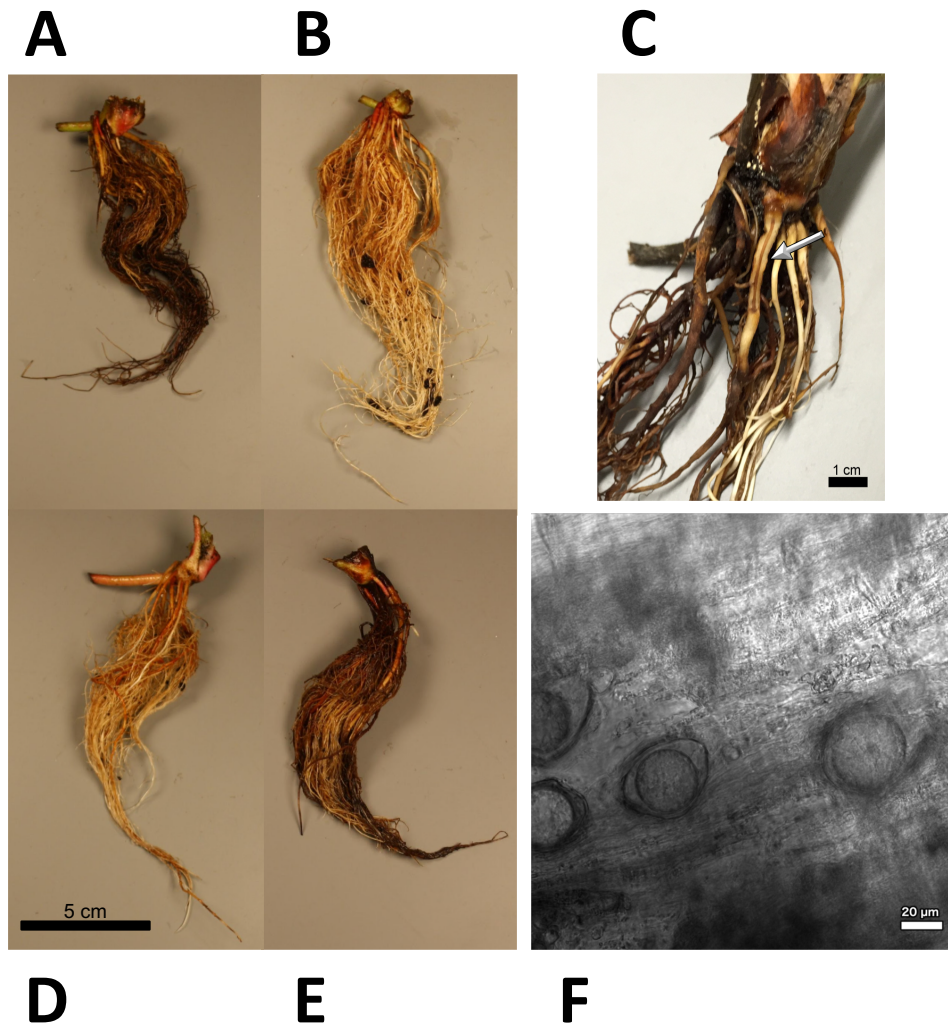
FIGURE 1 | Observed *Phytophthora fragariae* symptoms in the cultivated strawberry (*Fragaria × ananassa*). **(A,B,D,E)** Roots of *Fragaria × ananassa* harvested six weeks after inoculation with *Phytophthora fragariae* mycelial slurry. **(A)** Successful infection of the *P. fragariae* isolate NOV-27 (race CA2) on a susceptible 'Redgauntlet' plant (*Rpf2* only). **(B)** Unsuccessful infection of the *P. fragariae* isolate A4 (US4/UK2) on a resistant 'Redgauntlet' plant (*Rpf2* only). **(C)** Example of "red core" symptoms observed in 'Hapil' roots infected with BC-16, three weeks post inoculation. **(D)** Unsuccessful infection of the *P. fragariae* isolate NOV-27 (race CA2) on a resistant 'Allstar' plant (*Rpf1*, *Rpf2* and *Rpf3*). **(E)** Successful infection of the *P. fragariae* isolate A4 (race US4/UK2) on a susceptible 'Hapil' plant (no *Rpf* genes). **(F)** Example of BC-16 oospores observed in 'Hapil' roots, 3 weeks post inoculation, confirming infection.
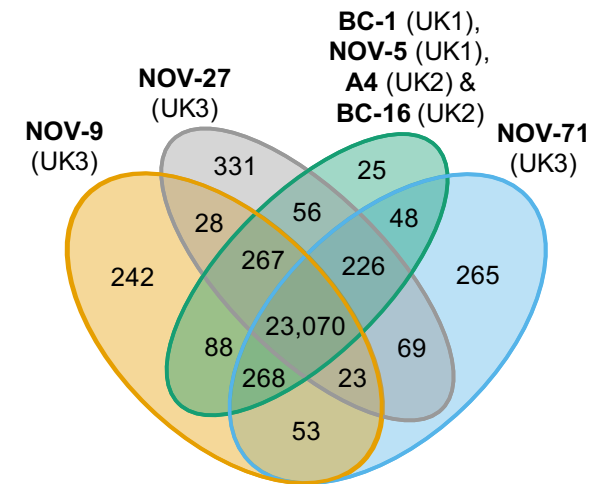
29

A

BC-1 (UK1) NOV-5 (UK1)

354 | 41 | 296

23,070

248 | 356

43
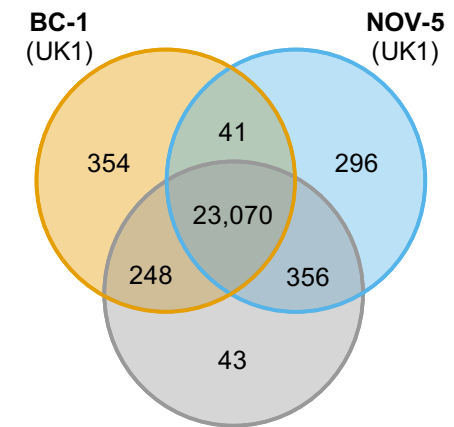
A4 (UK2), BC-16 (UK2), NOV-9 (UK3),
NOV-27 (UK3) & NOV-71 (UK3)

B

A4 (UK2) BC-16 (UK2)

269 | 115 | 2,246

23,070

1,639 | 273

84

BC-1 (UK1), NOV-5 (UK1), NOV-9 (UK3),
NOV-27 (UK3) & NOV-71 (UK3)

C

NOV-9 (UK3) NOV-27 (UK3) BC-1 (UK1), NOV-5 (UK1), A4 (UK2) & BC-16 (UK2) NOV-71 (UK3)

331 | 25
28 | 56 | 48
242 | 267 | 226 | 265
23,070
88 | 69
268 | 23
53

FIGURE 2 | Analysis of unique and expanded orthogroups for *Phytophthora fragariae* isolates of the UK1, UK2 and UK3 races did not lead to the identification of candidate avirulence genes. Orthology groups were identified by OrthoFinder (Emms and Kelly, 2015) and Venn diagrams were plotted using the VennDiagram R package (Chen and Boutros, 2011) in R (R Core Team, 2016). **(A)** Analysis focused on the *P. fragariae* isolates of race UK1: BC-1 and NOV-5 compared to isolates of races UK2 and UK3. **(B)** Analysis focused on the *P. fragariae* isolates of race UK2: A4 and BC-16 compared to isolates of races UK1 and UK3. **(C)** Analysis focused on the *P. fragariae* isolates of race UK3: NOV-5, NOV-27 and NOV-71 compared to isolates of races UK1 and UK2.

884
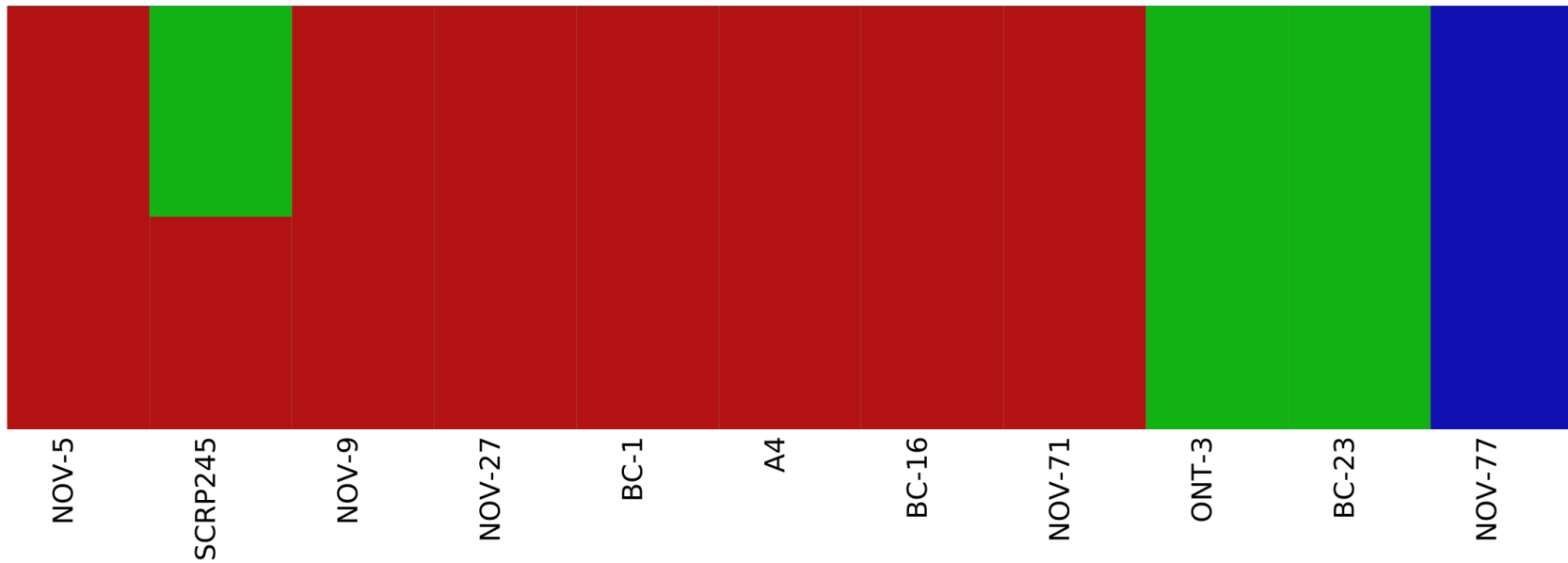
FIGURE 3 | Analysis of high quality, biallelic SNP sites split the isolates into three populations with SCRP245, potentially forming an ancestral or hybrid isolate between the UK1-2-3 population and the population represented by BC-23 and ONT-3. Distruct plot of fastSTRUCTURE (Raj et al., 2014) results carried out on all sequenced isolates of *Phytophthora fragariae*. Each colour represents a different population. Variant sites were identified by aligning Illumina reads of all the sequenced isolates to the reference assembly of the BC-16 isolate of *P. fragariae* with Bowtie 2 (Langmead and Salzberg, 2012) and analysis with the Genome Analysis Toolkit (GATK) haplotypecaller (McKenna et al., 2010). Sites were filtered with VCFtools (Danecek et al., 2011) and VCFlib (Garrison, 2012) to leave only high quality, biallelic SNP sites.

892
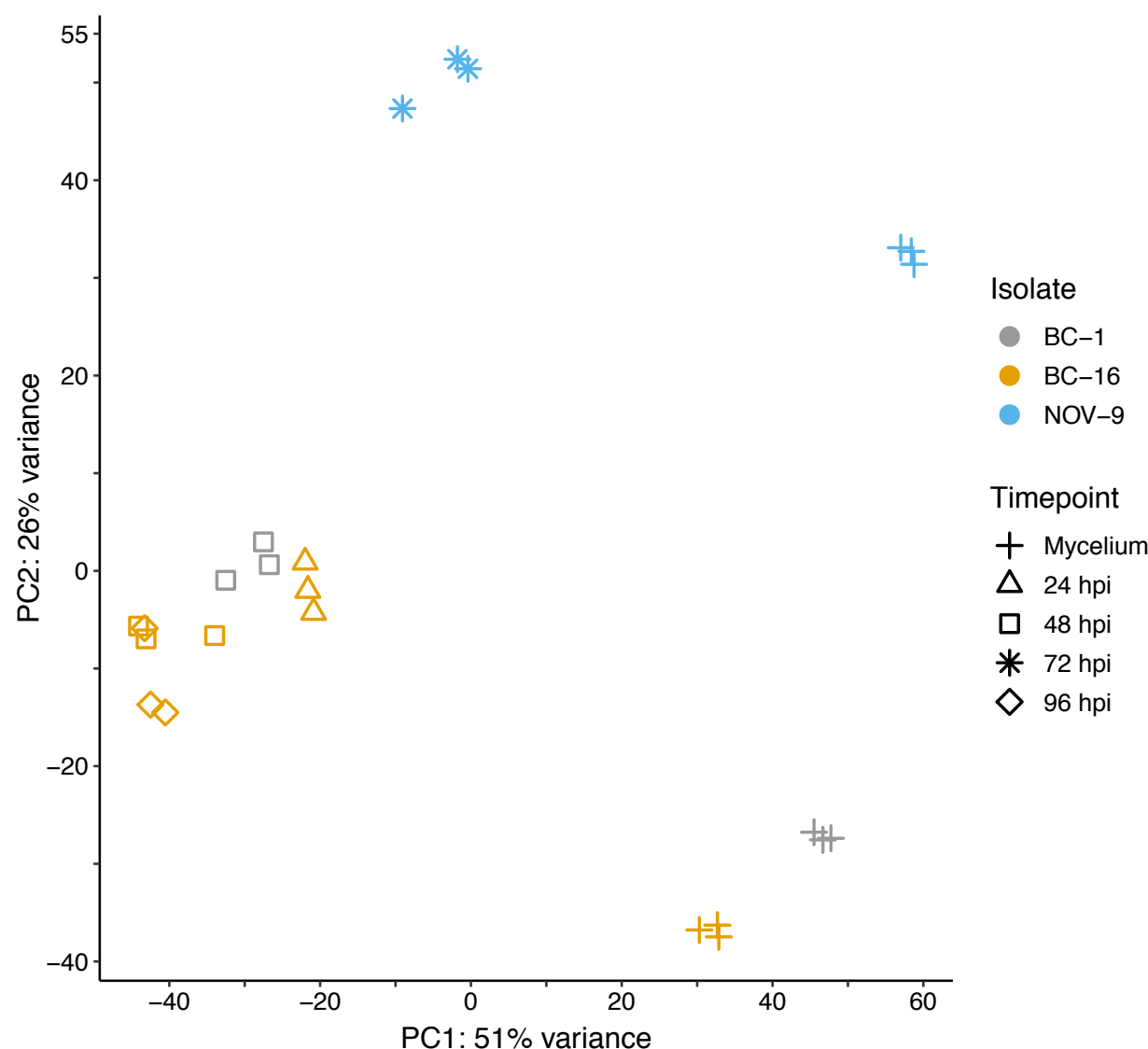
FIGURE 4 | Principal component analysis of expression data showed biological replicates of each timepoint grouped together, with clear separation observed for the BC-16 timepoints. RNA-Seq reads were aligned to the assembly of the BC-16 isolate of *Phytophthora fragariae* using STAR version 2.5.3a (Dobin et al., 2013). Predicted transcripts were then quantified with featureCounts version 1.5.2 (Liao et al., 2014) and differential expression was identified with the DESeq2 version 1.10.1 R package (Love et al., 2014). Following this, an rlog transformation of the expression data was plotted as a principal component analysis with R (R Core Team, 2016).

900
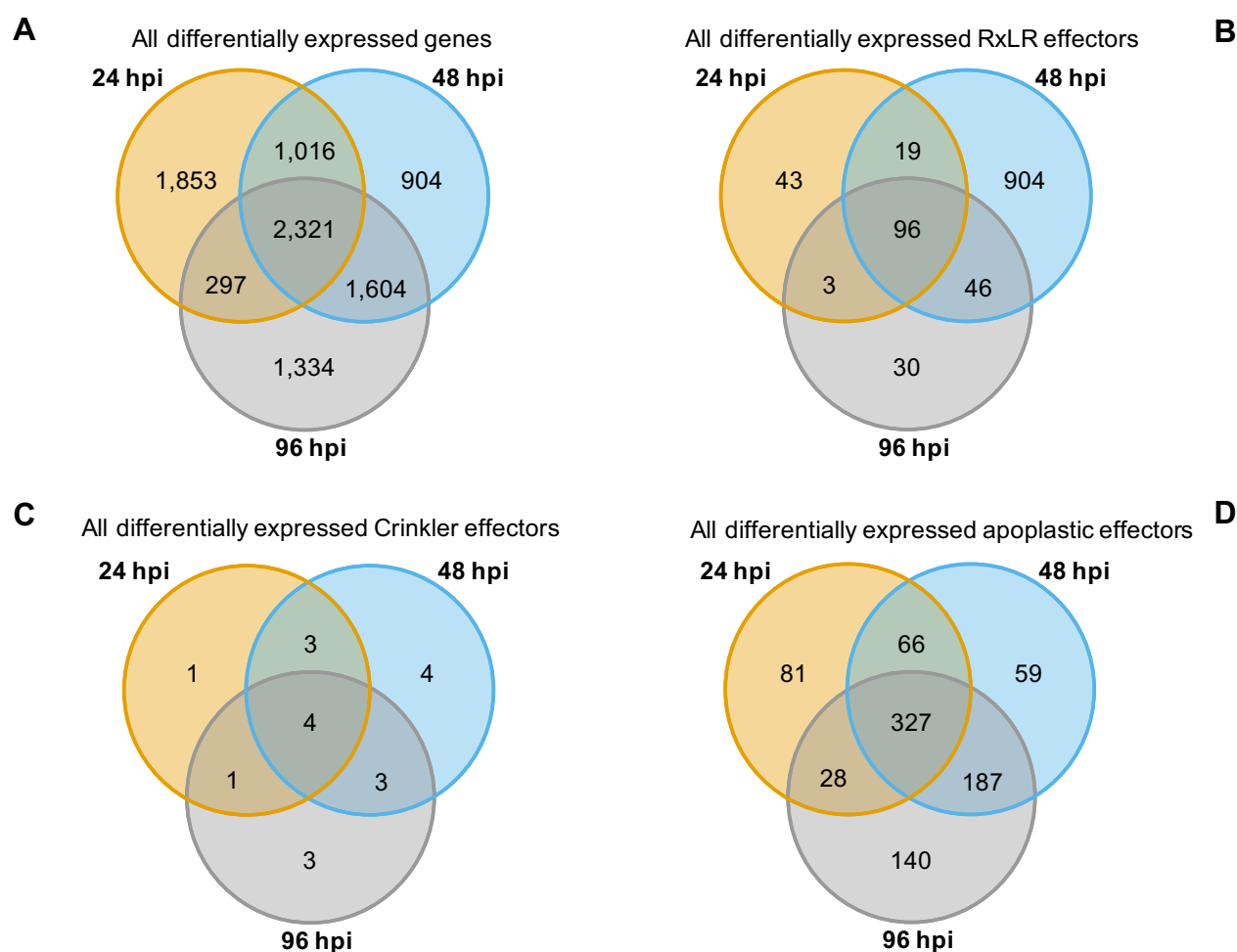
901 **FIGURE 5 | *In planta* RNA-Seq dataset captured changes during the progress of infection in the**
902 ***Phytophthora fragariae* BC-16 isolate.** RNA-Seq reads were aligned to the assembly of the BC-16
903 isolate of *P. fragariae* using STAR (Dobin et al., 2013). Predicted transcripts were then quantified
904 with featureCounts (Liao et al., 2014) and differential expression was identified with DESeq2 (Love
905 et al., 2014). Following this, Venn diagrams were plotted using the VennDiagram R package (Chen
906 and Boutros, 2011) in R (R Core Team, 2016). **(A)** All differentially expressed genes. **(B)** All
907 differentially expressed RxLR effectors. **(C)** All differentially expressed Crinkler effectors. **(D)** All
908 differentially expressed putative apoplastic effectors.

909
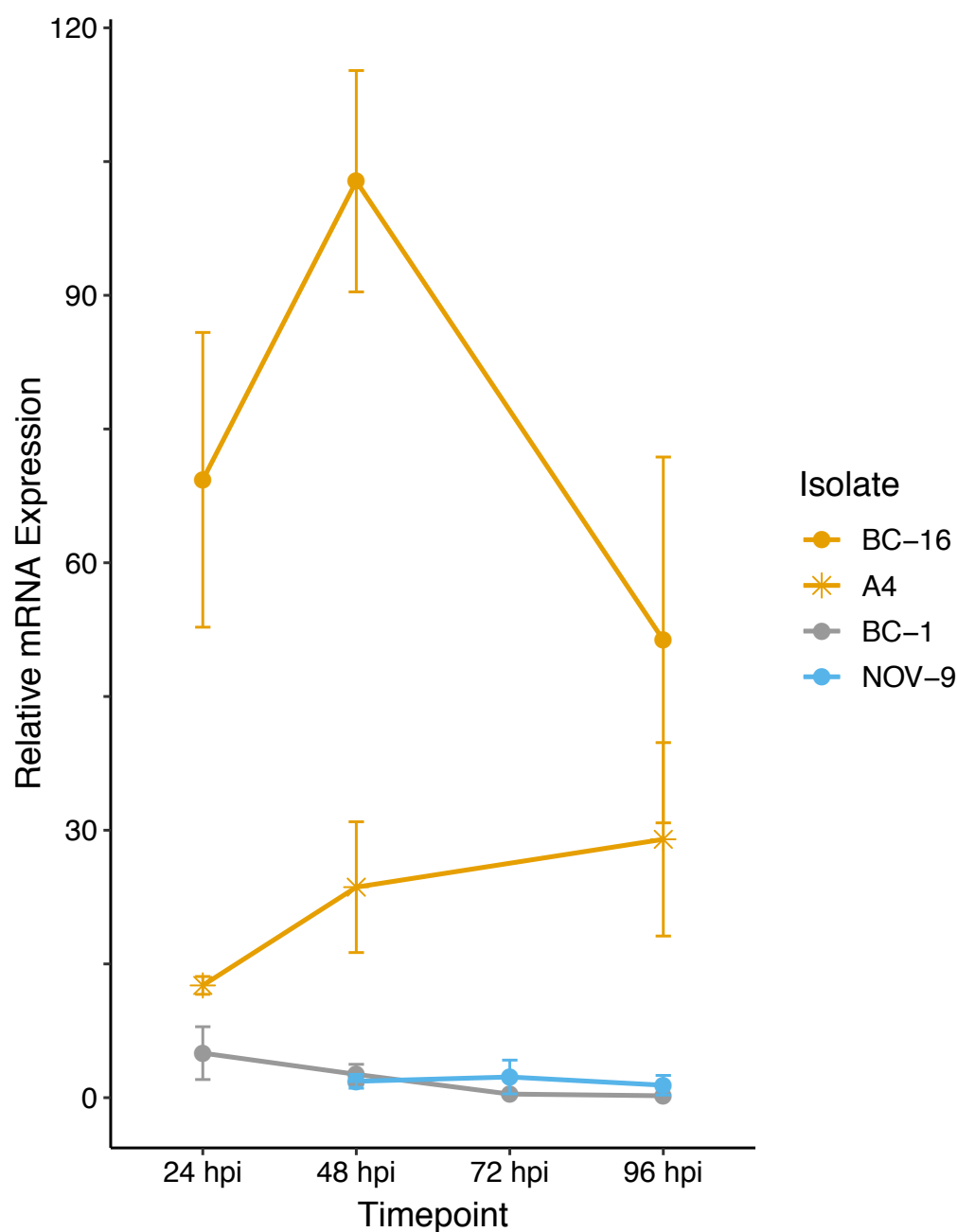
FIGURE 6 | *PfAvr2* **candidate PF003_g27513 is differentially expressed in** *Phytophthora fragariae* **UK-1-2-3 isolates.** Quantitative reverse transcription PCR of a strong candidate for the avirulence gene possessed by BC-16 and A4, but not BC-1 and NOV-9 (PF003_g27513.t1). Plots created by the ggplot2 R package (Wickham, 2016) in R version 3.4.3 (R core team, 2017).

A
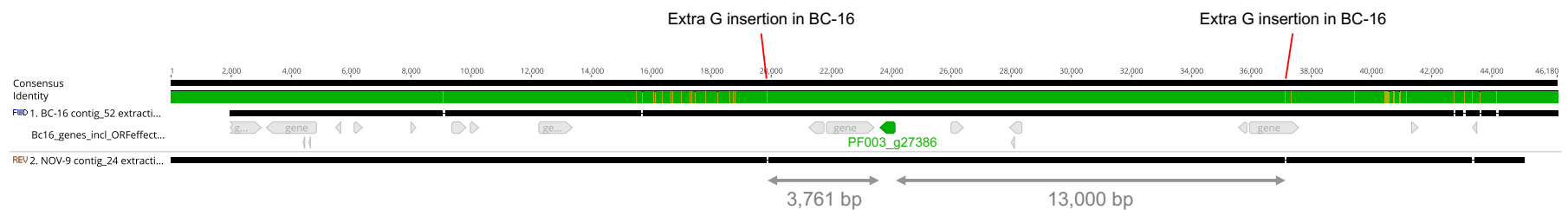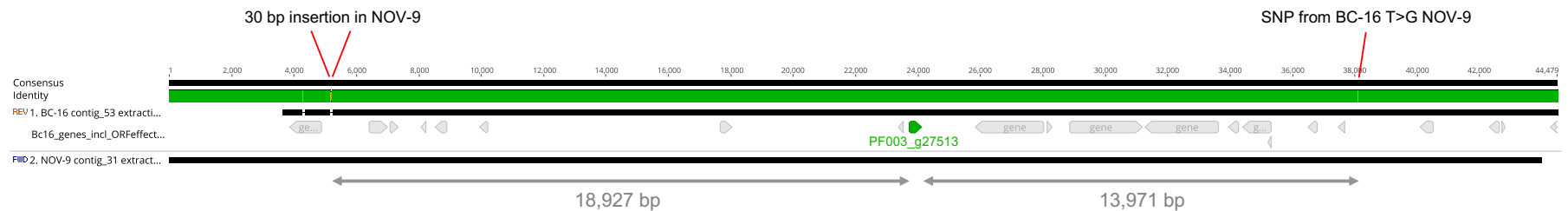
B

914

915 **FIGURE 7 | Differential expression of putative *PfAvr2* and *PfAvr3* is not due to sequence variation in *Phytophthora fragariae* BC-**

916 **16 (UK2) and NOV-9 (UK3) genomes.** Regions surrounding candidate avirulence genes, *PfAvr2* and *PfAvr3*, from BC-16 and NOV-9

917 aligned with MAFFT in Geneious R10 (Katoh et al., 2002; Katoh and Standley, 2013). (**A**) Putative *PfAvr2*, showing a 30 bp insertion in

918 the NOV-9 sequence upstream of PF003_g27513 and a T to G SNP in NOV-9 downstream of the gene of interest. (**B**) Putative *PfAvr3*,

919 showing an extra G insertion in BC-16 upstream of PF003_g27386 (an orthologue of PF009_g26267) and an extra G insertion in BC-16

920 3,761 bp downstream.

TABLES

TABLE 1 | Summary of *Phytophthora fragariae* and *Phytophthora rubi* isolates used in this study.

Isolate Name	Species	Location	Date Isolated	Isolated by	Pathogenicity Race
A4	*Phytophthora fragariae*	Unknown	17/12/2001	Unknown	US4
BC-1	*Phytophthora fragariae*	Commercial Strawberry Field, Delta, BC, Canada	05/01/2007	N. L. Nickerson	CA1 (UK1)
BC-16	*Phytophthora fragariae*	Commercial Strawberry Field, Ladner, BC, Canada	05/01/2007	N. L. Nickerson	CA3 (UK2)
BC-23	*Phytophthora fragariae*	Commercial Strawberry Field, Aldergrove, BC, Canada	30/01/2012	N. L. Nickerson	CA5
NOV-5	*Phytophthora fragariae*	Commercial Strawberry Field, Nine Mile River, Hants County, NS, Canada	17/12/2001	N. L. Nickerson	CA1
NOV-9	*Phytophthora fragariae*	Commercial Strawberry Field, Billtown, Kings County, NS, Canada	05/01/2007	N. L. Nickerson	CA2 (UK3)
NOV-27	*Phytophthora fragariae*	Commercial Strawberry Field, Cambridge Station, Kings County, NS, Canada	19/12/2001	N. L. Nickerson	CA2
NOV-71	*Phytophthora fragariae*	Commercial Strawberry Field, Middle Clyde River, Shelburne County, NS, Canada	05/01/2007	N. L. Nickerson	CA2
NOV-77	*Phytophthora fragariae*	Commercial Strawberry Field, Nine Mile River, Hants County, NS, Canada	30/01/2012	N. L. Nickerson	CA5
ONT-3	*Phytophthora fragariae*	Commercial Strawberry Field, Fort Erie, ON, Canada	05/01/2007	N. L. Nickerson	CA4
SCRP245	*Phytophthora fragariae*	Kent, England, UK	1945	Unknown	Unknown
SCRP249	*Phytophthora rubi*	Germany	1985	Unknown	1
SCRP324	*Phytophthora rubi*	Scotland, UK	1991	Unknown	1
SCRP333	*Phytophthora rubi*	Scotland, UK	1985	Unknown	3

TABLE 2 | *Phytophthora fragariae* race structure detected by three differential strawberry (*Fragaria × ananassa*) accessions and categorisation into UK race scheme.

Cultivar[a]	Mock	*Phytophthora fragariae* Isolate[b]						
		BC-1	**BC-16**	**NOV-9**	**A4**	**NOV-27**	**NOV-5**	**NOV-71**
Allstar[1,2,3]	$0^{4/4}$	$0^{8/8}$	$0^{7/7}$	$0^{4/4}$	$0^{3/4}$	$0^{2/3}$	$0^{3/3}$	$0^{4/5}$
Cambridge Vigour[2,3]	$0^{5/5}$	$+^{7/9}$	$0^{5/5}$	$0^{8/8}$	$0^{5/5}$	$0^{4/5}$	$+^{5/5}$	$0^{4/5}$
Hapil	$0^{12/12}$	$+^{10/10}$	$+^{10/10}$	$+^{10/10}$	$+^{4/5}$	$+^{5/5}$	$+^{3/5}$	$+^{5/5}$
Redgauntlet[2]	$0^{12/12}$	$+^{7/10}$	$0^{9/10}$	$+^{9/10}$	$0^{5/5}$	$+^{5/5}$	$+^{5/5}$	$+^{5/5}$
Deduced UK race	N/A	Race 1	Race 2	Race 3	Race 2	Race 3	Race 1	Race 3

[a] Known resistance genes in the *Fragaria × ananassa* cultivars.
[b] Number of replicates showing the recorded phenotype compared to the number of replicates tested; "+" representing a successful infection and "0" representing resistance.

TABLE 3 | Long read PacBio sequencing generated a highly contiguous *Phytophthora fragariae* BC-16 (UK2) reference genome. Assembly and annotation statistics compared to *Phytophthora sojae* P6497 (Tyler et al., 2006). Values in brackets include low confidence gene models from open reading frames.

	Phytophthora fragariae BC-16	*Phytophthora sojae* P6497
Assembly size (Mb)	90.97	82.60
Number of contigs	180	862
N50 (kb)	923.5	386.0
L50	33	61
Repeatmasked	38%	29%
Genes	37,049 (41,103)	26,584
RxLRs	486 (1,052)	350
CRNs	82 (85)	40
Apoplastic effectors	1,274 (4,757)	N/A

TABLE 4 | Comparable assembly statistics and gene predictions in resequenced isolates of *Phytophthora fragariae* and *Phytophthora rubi*.

	Phytophthora fragariae											*Phytophthora rubi*		
	A4	BC-1	BC-16	BC-23	NOV-5	NOV-9	NOV-27	NOV-71	NOV-77	ONT-3	SCRP245	SCRP249	SCRP324	SCRP333
Assembly Size (Mb)	79.08	79.10	90.97	78.26	78.99	79.43	79.75	78.37	78.80	79.06	77.84	77.79	77.91	77.82
Contig Number (≧ 500 bp)	13,446	11,556	180	13,191	13,531	11,801	12,489	12,212	13,321	13,265	13,231	14,023	13,946	13,679
N50 (kb)	18.2	21.8	923.5	18.2	17.9	21.5	19.4	20.2	18.9	18.8	18.2	16.6	16.9	16.9
L50	1,116	953	33	1,119	1,134	978	1,046	1,016	1,101	1,104	1,120	1,232	1,218	1,210
Repeatmasked	31%	31%	38%	31%	31%	31%	31%	31%	31%	31%	31%	31%	31%	30%
Genes[a]	30,180 (33,623)	30,375 (33,691)	37,049 (41,103)	29,960 (33,143)	30,248 (33,699)	29,986 (33,527)	30,600 (33,797)	29,708 (33,143)	30,099 (33,580)	30,180 (33,415)	30,202 (33,223)	31,458 (34,139)	30,235 (33,263)	32,623 (35,223)
Single-Copy BUSCO genes	274 (90%)	274 (90%)	266 (88%)	275 (91%)	273 (90%)	273 (90%)	273 (90%)	274 (90%)	272 (90%)	277 (91%)	273 (90%)	273 (90%)	274 (90%)	275 (91%)
Duplicated BUSCO genes	6 (2%)	6 (2%)	9 (3%)	5 (2%)	7 (2%)	6 (2%)	6 (2%)	6 (2%)	8 (2.5%)	7 (2%)	7 (2.5%)	8 (3%)	8 (3%)	7 (2%)
Fragmented BUSCO genes	6 (2%)	6 (2%)	5 (1.5%)	7 (2%)	6 (2%)	7 (2%)	7 (2%)	6 (2%)	6 (2%)	4 (1%)	7 (2.5%)	3 (1%)	3 (1%)	3 (1%)
Missing BUSCO genes	17 (6%)	17 (6%)	23 (7.5%)	16 (5%)	17 (6%)	17 (6%)	17 (6%)	17 (6%)	17 (5.5%)	15 (5%)	16 (5%)	19 (6%)	18 (6%)	18 (6%)

[a] Values in brackets include low confidence gene models from open reading frames.

TABLE 5 | Effector gene predictions in resequenced isolates of *Phytophthora fragariae* and *Phytophthora rubi*.

| | *Phytophthora fragariae* | | | | | | | | | | | *Phytophthora rubi* | | |
	A4	BC-1	BC-16	BC-23	NOV-5	NOV-9	NOV-27	NOV-71	NOV-77	ONT-3	SCRP245	SCRP249	SCRP324	SCRP333
Secreted proteins[a]	3,637	3,601	4,217	3,611	3,626	3,637	3,690	3,633	3,620	3,658	3,581	3,697	3,683	3,832
RxLR HMM[b]	194	194	218	188	196	186	183	191	166	191	196	197	195	207
RxLR-EER Regex[c]	178	184	208	176	186	174	172	182	150	178	185	188	176	188
RxLR Regex	371	367	445	364	370	356	369	374	341	367	370	363	350	359
Final RxLR effectors[d]	410 (935)	405 (919)	486 (1,052)	402 (928)	408 (918)	397 (951)	405 (899)	412 (931)	378 (934)	403 (898)	407 (882)	407 (882)	395 (861)	410 (826)
CRN LFLAK HMM[c]	85	83	114	86	84	82	87	90	86	90	90	156	93	154
CRN DWL HMM[c]	95	87	121	96	91	96	93	101	83	90	87	139	102	142
Final CRNs[d,e]	55 (68)	53 (59)	82 (87)	55 (62)	53 (67)	50 (61)	57 (63)	59 (71)	62 (75)	61 (74)	60 (68)	128 (132)	71 (85)	128 (134)
Apoplastic effectors[d,f]	991 (3,896)	1,002 (3,798)	1,274 (4,757)	980 (3,630)	986 (3,913)	1,007 (3,983)	1,011 (3,708)	1,007 (3,911)	1,010 (3,922)	982 (3,709)	984 (3,522)	1,017 (3,266)	1,059 (3,607)	1,090 (3,268)

[a] SignalP: Nielsen et al., 1997; Bendtsen et al., 2004; Petersen et al., 2011 and Phobius: Käll et al., 2007.
[b] Whisson et al., 2007.
[c] Armitage et al., 2018.
[d] Values in brackets include low confidence gene models from open reading frames.
[e] Both LFLAK and DWL HMM models present (Armitage et al., 2018).
[f] ApoplastP: Sperscneider et al., 2018.

TABLE 6 | Conserved putative core *Phytophthora fragariae* RxLR effector candidates important for pathogenicity on strawberry (*Fragaria × ananassa*) from isolates BC-1, BC-16 and NOV-9. Conserved RxLR candidates in the 50 highest expressed genes *in planta* with a log fold change (LFC) of ≥3, based on comparison to respective mycelium. The BC-16 24 hour post inoculation (hpi) timepoint was used for BC-16.

| | | Fragments Per Kilobase of transcript per Million mapped reads (FPKM) | | | | | | | | |
| Orthogroup | BC-16 gene ID | BC-1 (UK1) | | BC-16 (UK2) | | | | NOV-9 (UK3) | | Avr homology |
		Mycelium	48 hpi	Mycelium	24 hpi	48 hpi	96 hpi	Mycelium	72 hpi	
OG0010423	PF003_g35418	94	5,354	192	6,578	4,986	2,961	12	3,868	
OG0018019	PF003_g6480	241	3,544	235	2,113	1,977	1,717	231	2,501	
OG0011458	PF003_g16448	4	2,899	4	4,656	2,108	1,090	7	1,699	*P. sojae Avr1b*[a]
OG0021012	PF003_g16234	36	1,345	31	1,181	827	674	23	737	

[a] Top hit from GenBank tblastn search is AF449623, *Phytophthora sojae Avr1b* (Shan et al., 2004).

SUPPLEMENTARY MATERIAL

A

B
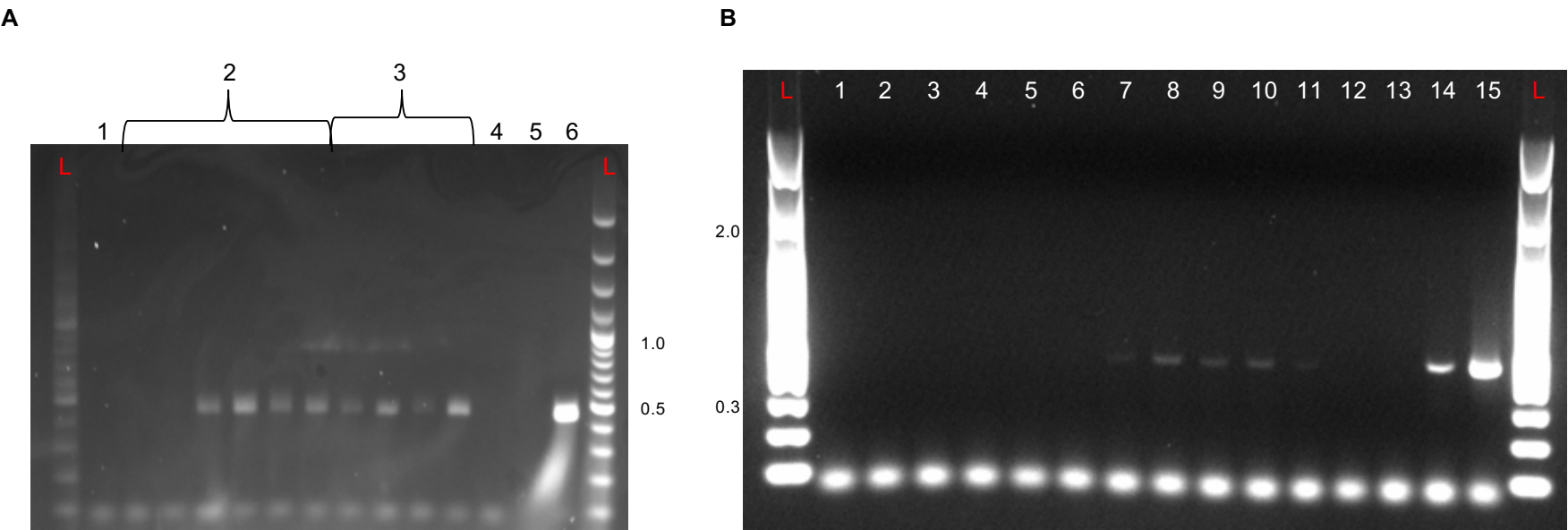
922

SUPPLEMENTARY FIGURE S1 | Agarose gel electrophoresis of RT-PCR reactions on representative samples from inoculation time course experiments on the 'Hapil' cultivar of *Fragaria* × *ananassa*. A: Gel of samples from an inoculation time course experiment with the BC-16 isolate of *Phytophthora fragariae*. **L:** 100 bp Plus Ladder (ThermoFisher Scientific, Waltham, MA, USA) sizes listed in kb. **1:** Mock inoculated *Fragaria* × *ananassa* cultivar 'Hapil' plant. **2:** Time course of inoculated plants with stream water used as the flooding solution. Time points from left to right: 24 hpi, 48 hpi, 96 hpi, 144 hpi, 192 hpi and 240 hpi. **3:** Time course of inoculated plants with Petri's solution used as the flooding solution. Time points from left to right: 24 hpi, 48 hpi, 96 hpi and 144 hpi. **4:** dH2O control. **5:** 'Flamenco' gDNA control. **6:** BC-16 gDNA control. **B**: Gel of samples from an inoculation time course experiment with the BC-1 and NOV-9 isolates of *P. fragariae*. **L**: 100 bp plus ladder from New England Biolabs, sizes listed in kb. PCR templates: **1**: Uninoculated plant cDNA. **2**: NOV-9 12 hours post inoculation (hpi) cDNA. **3**: BC-1 12 hpi cDNA. **4**: NOV- 9 24 hpi cDNA. **5**: BC-1 24 hpi cDNA. **6**: NOV-9 48 hpi cDNA. **7**: BC-1 48 hpi cDNA. **8**: NOV-9 72 hpi cDNA. **9**: BC-1 72 hpi cDNA. **10**: NOV-9 96 hpi cDNA. **11**: BC-1 96 hpi cDNA. **12**: dH2O. **13**: gDNA from a *F.* × *ananassa* cultivar 'Hapil' plant. **14**: gDNA from BC-16 mycelium. **15**: cDNA from BC-16 mycelium.
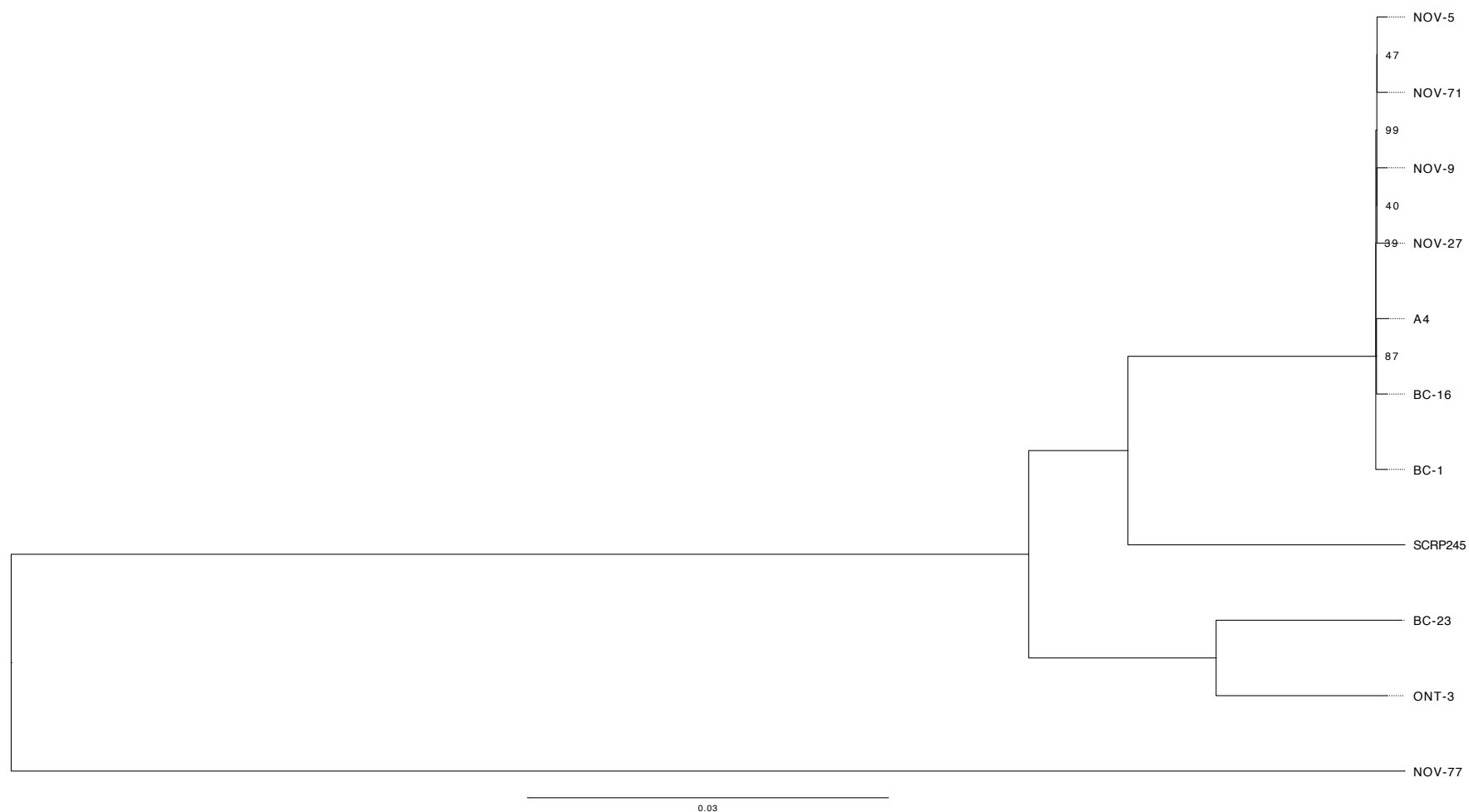
934

935 **SUPPLEMENTARY FIGURE S2 |** *Phytophthora fragariae* **isolates separate into distinct clades.** Neighbour joining tree based on high

936 quality, biallelic SNP sites, node labels represent the number of bootstrap replicates supporting the node; only values less than 100 are

937 shown.

938
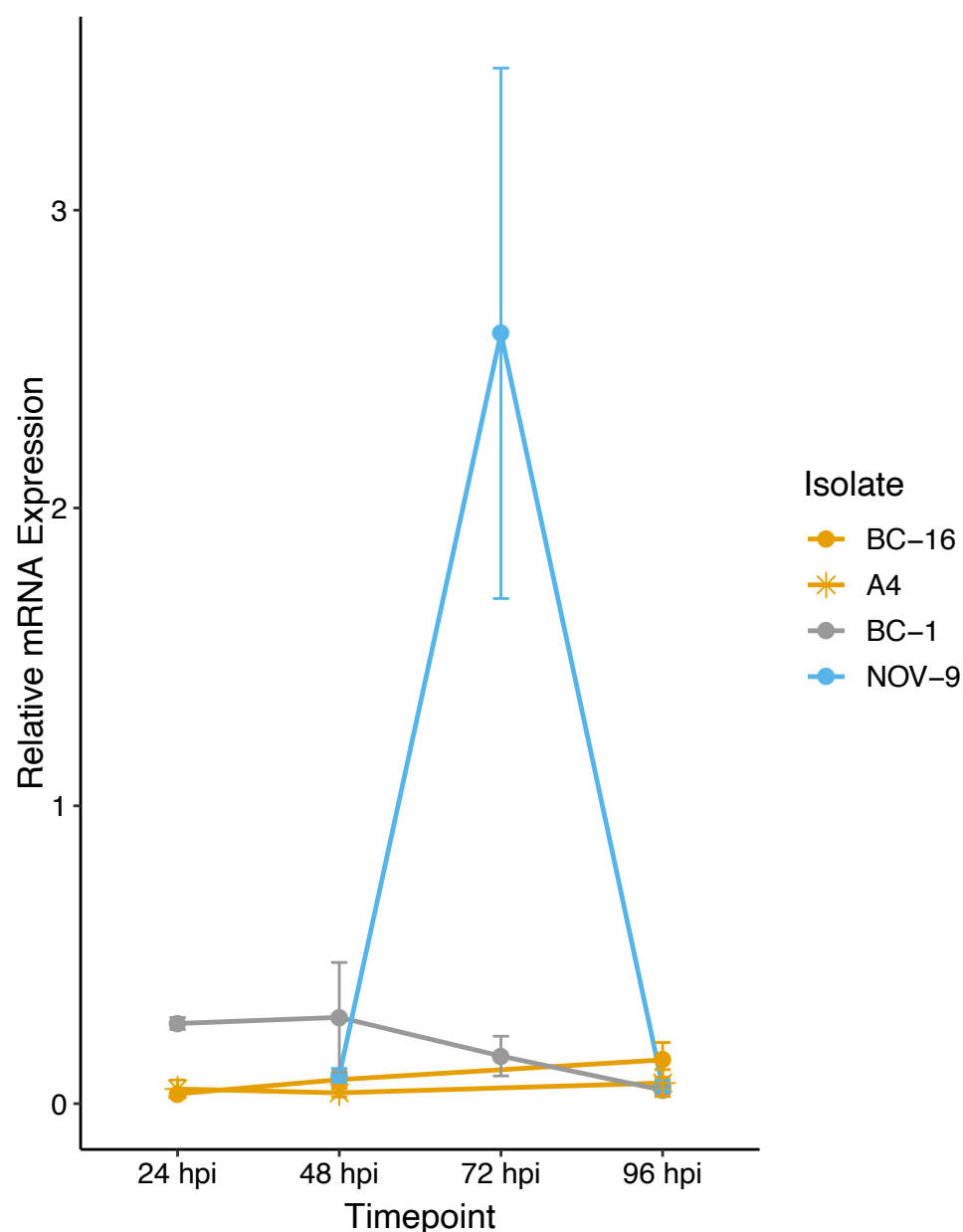
SUPPLEMENTARY FIGURE S3 | *PfAvr3* **candidate PF009_g26276 is differentially expressed**

in *Phytophthora fragariae* **UK-1-2-3 isolates.** Quantitative reverse transcription PCR of a candidate

for the avirulence gene possessed by NOV-9, but not BC-1, BC-16 and A4 (PF009_g26276.t1). Plots

created by the ggplot2 R package (Wickham, 2016) in R version 3.4.3 (R core team, 2017).

SUPPLEMENTARY TABLES

SUPPLEMENTARY TABLE S1 | Primers used in this study. Primers supplied by IDT (Leuven, Belgium).

Primer Name	Target	Gene Name	BC-16 Gene ID	Primer Sequence	Length (bp)	Reference
Pf_Btub_F	RT-PCR	β-tubulin	PF003_g4288.t1	5'-GGATAACGAGGCCCTGTACG-3'	440	This Study
Pf_Btub_R				5'-TGTTGTTGGGGATCCACTCG-3'		
WS41_163F	Housekeeping	WS41	PF003_g28439.t1	5'-ATCGTGCTGTACCTGGGC-3'	156	This Study
WS41_318R				5'-GATCTCGCTGGGCTTGAAGG-3'		
Btub_44F	Housekeeping	β-tubulin	PF003_g4288.t1	5'-CCGCGCCCGTACAGCAAC-3'	109	This Study
Btub_152R				5'-TCGGAGATGACTTCCCAGAACTTG-3'		
cAvr2_65F	Candidate Race 2 *Avr* Gene	Candidate *PfAvr2*	PF003_g27513.t1	5'-TGTCAAAGGCCGATCAGAGC-3'	180	This Study
cAvr2_244R				5'-CGAACAAACTATCCACACCAGC-3'		
cAvr3_F	Candidate Race 3 *Avr* Gene	Candidate *PfAvr3*	PF003_g27386.t1	5'-ACAAGATGGACCCGAACCTCAT-3'	209	This Study
cAvr3_R				5'-CAACCTCCTGACAGCTCCTTCAAC-3'		
U16SRT-F	Inter-plate calibrator	16S	N/A	5'-ACTCCTACGGGAGGCAGCAGT-3'	180	Clifford et al., 2012
U16SRT-R				5'-TATTACCGCGGCTGCTGGC-3'		

SUPPLEMENTARY TABLE S2 | Details of expression of genes surrounding putative *PfAvr2* (PF003_g27513).

| | Orthogroup | BC-16 gene ID | Fragments Per Kilobase of transcript per Million mapped reads (FPKM) | | | | | | | |
| | | | BC-1 | | BC-16 | | | | NOV-9 | |
			Mycelium	48 hpi	Mycelium	24 hpi	48 hpi	96 hpi	Mycelium	72 hpi
	OG0003811	PF003_g27515	0	0	0	0	0	0	0	0
	OG0000375	PF003_g27514	476	546	11	248	260	206	58	80
Putative *PfAvr2*	**OG0026610**	**PF003_g27513**	**0**	**0**	**1**	**9,392**	**6,263**	**3,075**	**0**	**33**
	OG0000960	PF003_g27512	3	1	0	0	0	1	2	2
	OG0036362	PF003_g27511	0	0	0	0	0	0	--	--

SUPPLEMENTARY TABLE S3 | Details of expression of genes surrounding putative *PfAvr3* (PF003_g27386/PF009_g26276).

	Orthogroup	BC-16 gene ID	Fragments Per Kilobase of transcript per Million mapped reads (FPKM)							
			BC-1		BC-16				NOV-9	
			Mycelium	48 hpi	Mycelium	24 hpi	48 hpi	96 hpi	Mycelium	72 hpi
	OG0002229	PF003_g27388	0	0	0	0	0	0	0	0
	OG0003130	PF003_g27387	0	0	0	0	0	0	0	0
Putative *PfAvr3*	**OG0018589**	**PF003_g27386**	**17**	**6**	**10**	**12**	**4**	**4**	**16**	**199**
	OG0018588	PF003_g27385	38	33	26	36	64	78	29	61
	OG0018587	PF003_g27384	0	0	0	0	0	0	1	1

943 **SUPPORTING TABLES**

944 **SUPPORTING CANDIDATE TABLE | Gene names of all genes identified as putative candidate**

945 **avirulence genes for *Phytophthora fragariae* UK1, UK2 and UK3.**

946 Gene names are listed with respect to the isolate for which they are described as candidate avirulence

947 genes.

948

949 **SUPPORTING ANNOTATION TABLE | Details of all predicted genes in *Phytophthora***

950 ***fragariae* UK2 isolate BC-16.**